European Journal of Medicinal Chemistry 75 (2014) 354–374

Contents lists available at ScienceDirect

European Journal of Medicinal Chemistry

journal homepage: http://www.elsevier.com/locate/ejmech

Original article

Structure–activity study leading to identification of a highly active thienopyrimidine based EGFR inhibitor

Steffen Bugge [a], Svein Jacob Kaspersen [a], Synne Larsen [a], Unni Nonstad [b], Geir Bjørkøy [b,c], Eirik Sundby [d], Bård Helge Hoff [a,*]

[a] Department of Chemistry, Norwegian University of Science and Technology, Høgskoleringen 5, NO-7491 Trondheim, Norway
[b] Centre of Molecular Inflammation Research, Norwegian University of Science and Technology, Prinsesse Kristinas Gate 1, NO-7491 Trondheim, Norway
[c] Sør-Trøndelag University College, Erling Skjalgssons Gate 1, NO-7004 Trondheim, Norway
[d] Sør-Trøndelag University College, E.C. Dahls Gate 2, NO-7004 Trondheim, Norway

ARTICLE INFO

Article history:
Received 28 November 2013
Received in revised form
16 January 2014
Accepted 19 January 2014
Available online 31 January 2014

Keywords:
Thienopyrimidine
Benzylamine
Suzuki-coupling
EGFR-TK
SAR
Erlotinib

ABSTRACT

Based on the thieno[2,3-*d*]pyrimidine scaffold, a series of new 4-amino-6-aryl thienopyrimidines have been prepared and evaluated as EGFR tyrosine kinase inhibitors. The *in vitro* activity was found to depend strongly on the substitution pattern in the 6-aryl ring, the stereochemistry, and the basicity at the secondary 4-amino group. A stepwise optimization by combination of active fragments led to the discovery of three structures with EGFR $IC_{50} < 1$ nM. The most potent drug candidate had an IC_{50} of 0.3 nM towards EGFR and its mutants L858R and L861Q. Studies using human cancer cell lines and an EGFR-L858R reporter cell system revealed good cellular potency, verifying the identified thienopyrimidines as promising lead structures.

1. Introduction

Epidermal growth factor receptor tyrosine kinase (EGFR-TK) represents a major target in small molecular cancer therapy [1–3]. This transmembrane receptor contains an extracellular binding site for epidermal growth factors (EGF), and an intracellular tyrosine kinase domain. Binding of EGF induces dimerization and thereby activation of the kinase domain [2]. Monoclonal antibodies such as Cetuximab and Panitumumab interfere with ligand binding and/or activation of the extracellular kinase domain [4,5], and some monoclonal antibodies might in addition trigger immune responses [1,6]. In contrast, properly designed low molecular weight compounds are attractive as inhibitors of the intracellular kinase domain, since they also can inhibit ligand independent mutant receptors, and for their more moderate cost profile. Examples of ATP competitive inhibitors on the marked include Gefitinib, Erlotinib, Lapatinib and Vandetanib, which all are based on a central quinazoline core, see Fig. 1. Both intra- and extracellular inhibitors have the effect of down regulating downstream signalling events and thereby the growth and survival of the tumour [7].

X-ray structural data is available for EGFR-TK co-crystallized with quinazoline based inhibitors [8–11], and also the pyrrolopyrimidine AEE-788 [10]. The ATP binding site is in a cleft formed by the C- and N terminal loops of the kinase. The X-ray structures indicate that the inhibitors affinity for the binding site originates from hydrogen bonding between N-1 of the pyrimidine to the main chain NH of Met793 [10]. For AEE-788 a hydrogen bond interaction was observed between N-3 and Thr854 via a bridged water molecule [10].

The 4-amino group is directed in a small hydrophobic pocked allowing for stabilization by dispersion forces. None of the X-ray studies have indicated that the amine function at C-4 is involved in binding. The substituents present at the benzo, pyrrolo or thieno

Abbreviations: ATP, adenosine triphosphate; BEI, binding efficiency; cGMP, cyclic guanosine monophosphate; DFG, Asp-Phe-Gly; EGF, epidermal growth factor; EGFR-TK, epidermal growth factor receptor tyrosine kinase; HER, human epidermal growth factor receptor; LE, ligand efficacy; LLE, lipophilic ligand efficiency; LELP, lipophilicity corrected ligand efficiency; MIDA, *N*-methyliminodiacetic acid; SEI, surface efficiency index; IL-3, interleukin-3; TP53, tumour protein p53.

* Corresponding author. Tel.: +47 73593973; fax: +47 73544256.
E-mail addresses: Steffen.Bugge@chem.ntnu.no (S. Bugge), Svein.Jacob.Kaspersen@chem.ntnu.no (S.J. Kaspersen), synnelar@gmail.com (S. Larsen), unni.nonstad@ntnu.no (U. Nonstad), geir.bjorkoy@hist.no (G. Bjørkøy), eirik.sundby@hist.no (E. Sundby), bard.helge.hoff@chem.ntnu.no, bard.hoff@online.no (B.H. Hoff).

0223-5234/$ – see front matter © 2014 Elsevier Masson SAS. All rights reserved.
http://dx.doi.org/10.1016/j.ejmech.2014.01.042

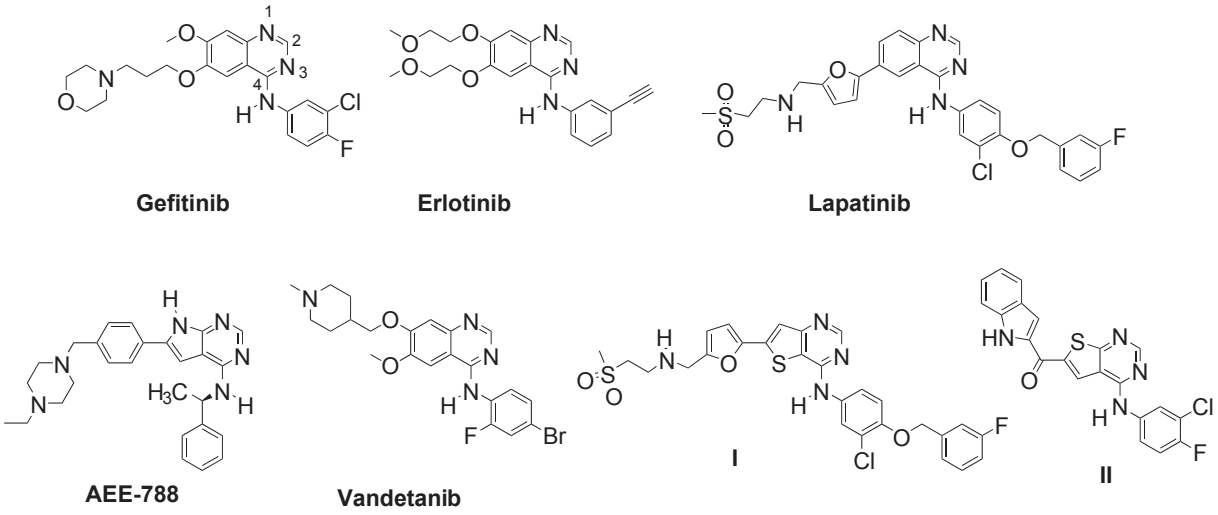

Fig. 1. Structure of some potent EGFR inhibitors.

fragment of the heterocycle, often called "solubilizing tail", are directed towards the entrance of the ATP binding site.

Our laboratory has recently investigated 4-benzylamine substituted pyrrolopyrimidines as EGFR tyrosine kinase ATP competitive inhibitors [12]. Herein we report an extension of this research by employing thieno[2,3-*d*]pyrimidine as the scaffold. Thienopyrimidines in general have become an interesting structural element in development of pharmaceutical compounds [13,14], and have among others been evaluated as cGMP phosphodiesterase inhibitors [15], anti-viral agents [16], but also as kinase inhibitors and potential anti-cancer agents [17–20]. Research on thienopyrimidine analogues of Lapatinib such as **I**, and compound **II** both revealed low nanomolar potency towards EGFR [21,22]. In addition, irreversible thienopyrimidine based EGFR inhibitors have been developed [23]. Based on an efficient synthetic route we have synthesized a series of new chiral thieno[2,3-*d*]pyrimidine derivatives and evaluated their efficiency as EGFR-TK inhibitors.

2. Result and discussion

2.1. Design of the inhibitors

Our intention was to use the thienopyrimidine as a substitute for quinazoline or pyrrolpyrimidine for construction of EGFR-TK inhibitors (Fig. 2), a strategy known as scaffold hopping. As compared to the previously reported active pyrrolopyrimidines [12,24], the thienopyrimidines lack the N–H unit as presented by the pyrrole, but the X-ray structure of AEE-788 (Fig. 1) bond to EGFR did not indicate the pyrrole nitrogen as important in binding [10]. Also, the longer S–C bond in the thiophene fragment as compared to the pyrrole could affect EGFR-ligand binding, and therefore could require a different substitution pattern. Herein, the 6-aryl group has been used as a scaffold in scanning for favourable/unfavourable lipophilic, dipolar and hydrogen bond interactions. Besides the more direct binding interactions, long range electronic effects to the pyrimidine nitrogens might also play a role. Moreover, the reported X-ray studies have not indicated any clear role for the C-4 amino group in binding. We have also addressed this issue by evaluating the performance of designed model compounds.

2.2. Synthesis

To investigate the effect of structural variations in Fragment A (Fig. 2) on EGFR inhibitory potency, a series of target molecules were constructed as shown in Scheme 1.

6-Bromo-4-chlorothieno[2,3-*d*]pyrimidine (**1**), synthesized in house by a four step procedure in multi-gram scale [25], was reacted with (*R*)-1-phenylethylamine ((*R*)-**2**) giving (*R*)-**3**. The following Suzuki couplings using $Pd(PPh_3)_4$ gave the derivatives **5**, mostly in >70% yield. As compared to our previous study [25], tuning of the reaction conditions by lowering the reaction temperature and the amount of catalyst, gave easier purifications. Loss in yield in these reactions was mainly due to purification issues rather than low conversions, as some cross-coupling of the boronic acids occurred.

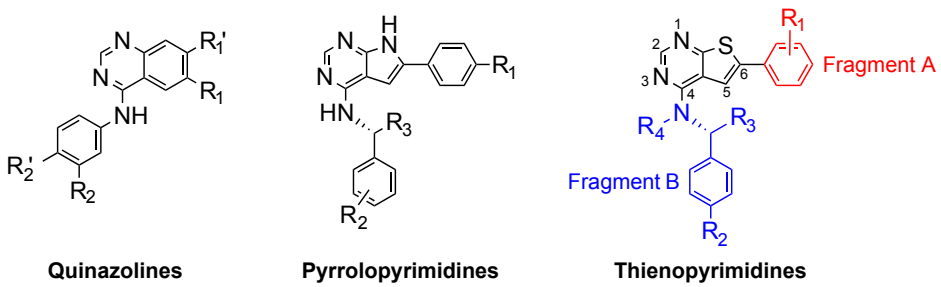

Fig. 2. Structure of benzo-, pyrrolo- and the investigated thienopyrimidines.

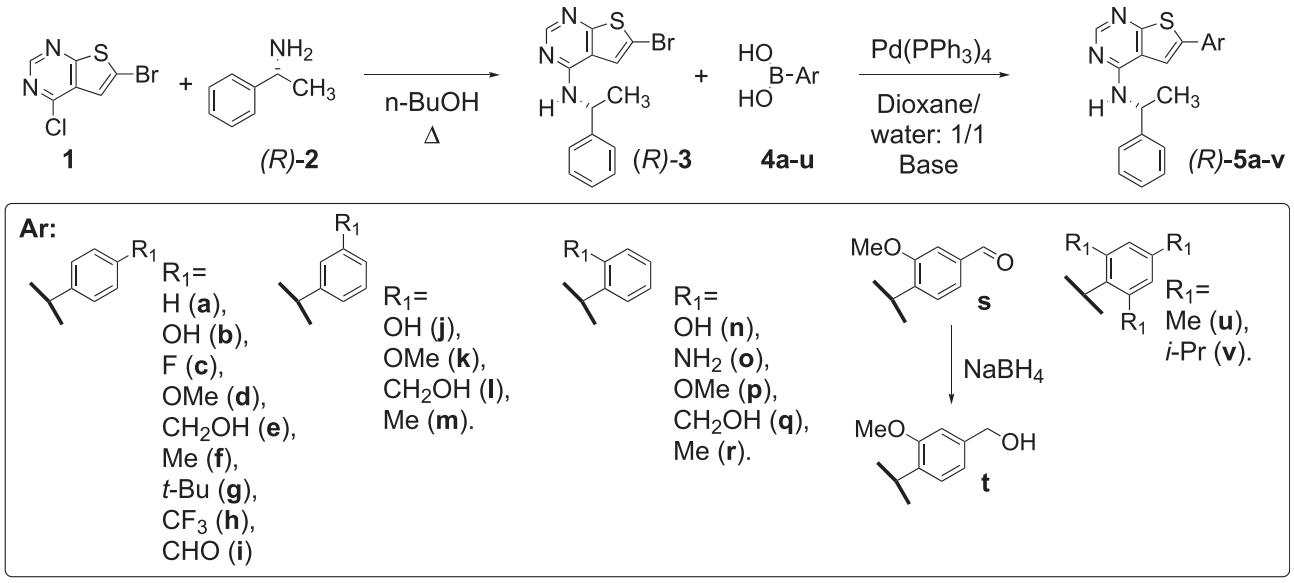

Scheme 1. Synthesis of the thienopyrimidines (*R*)-**5a**–**v**.

We were also able to couple the sometimes demanding 2-aminophenylboronic acid in 84% yield. In selected cases the corresponding *N*-methyliminodiacetic acid (MIDA) boronate esters were used, with $Pd(OAc)_2$ and SPhos as the catalyst system, with somewhat lower yields. During optimization of EGFR-TK activity, compound (*R*)-**5s** was synthesized, which by sodium borohydride reduction gave access to the disubstituted derivative (*R*)-**5t**.

In order to investigate the effect of structural variation in Fragment B on EGFR-TK inhibitory potency, a series of related derivatives **25**–**33** were prepared using similar chemistry, Scheme 2. The amination reactions proceeded as for (*R*)-**3** in every case except when using the monofluoroamine, (*rac*)-**12**, which was unstable at higher temperatures. Thus, the reaction was performed at 50 °C for 72 h. The following Suzuki coupling on **15**–**23** gave complete conversion in every case, but fine tuning of the work-up and purification was needed to fully purify the compounds. Selected derivatives were also prepared by an alternative route via **24a** [25] and **24c**. However, due to a moderate selectivity in the Suzuki coupling the yields were somewhat low. The building blocks **24a** and **c** were then transformed to compounds (*S*)-**5a**, (*R*)-**5c** and (*R*)-**25c**, through standard thermal amination chemistry. The analogue ether (*rac*)-**36n** was synthesized from **1** and racemic 1-phenylethanol (**34**) with sodium hydride as base forming the ether (*rac*)-**35**, which was converted to compound (*rac*)-**36n** in the usual manner.

The purity of all compounds was evaluated by HPLC. To verify that the enantiomeric excess of the products were not affected by the chemistry, a chiral analysis was developed for **5a** using a Lux 5u Cellulose HPLC column. Both (*R*)- and (*S*)-**5a** were measured to have an *ee* of 99%, indicating no racemization.

2.3. EGFR inhibitory potency

As compared to the corresponding pyrrolopyrimidine **III** [12], analysed by the same assay (Supporting information Table S1), a significant drop in EGFR-TK potency was noticed for the structurally related thienopyrimidine (*R*)-**5a**, see Fig. 3.

We therefore took on a stepwise approach where the effects of the 6-aryl group (Fragment A) and the 4-amino group (Fragment B) on EGFR-TK inhibitory potency were separately investigated and optimized.

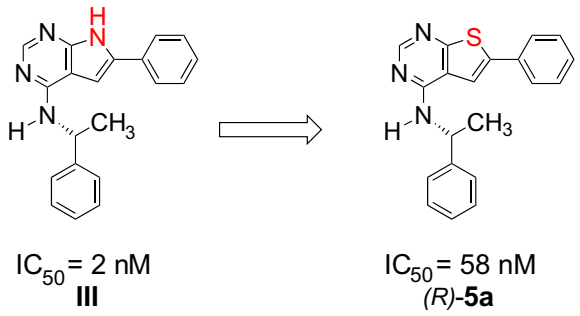

Fig. 3. Scaffold hopping by heterocyclic replacement used for discovery of new EGFR-TK inhibitors.

2.3.1. Structural variations in Fragment A

The initial plan to improve potency was to "scan" for possible hydrogen bonding interactions and lipophilic contacts. Substituents varied in the 6-aryl group (Fragment A) were OH and CH_2OH with the idea of mimicking the hydrogen bonding ability of the pyrrole; methyl groups to search for possible lipophilic contacts and as a control of any conformational effects; and methoxy substituents as possible hydrogen bond acceptors. Later, additional compounds were included to refine the structure–activity study. The results in terms of IC_{50} for the *mono* substituted derivatives **5a**–**r**, and the trisubstituted compounds **5u**, **v** are shown in Fig. 4.

As compared to the starting point, (*R*)-**5a**, the potency was increased from 58 nM to 7 and 9 nM by introducing a *para* hydroxymethyl group (comp. (*R*)-**5e**) or an *ortho* methoxy group (comp. (*R*)-**5p**). Compound (*R*)-**5l** having a *meta* hydroxymethyl group also showed promising activity (9 nM).

The major substituent effects observed are visualized in Fig. 5. Methyl substitution decreased the potency in any position. For compounds having the phenolic- or the methoxy group, the activity increase in the order *para* < *meta* < *ortho*. This indicated that a hydrogen bond acceptor is beneficial in the *ortho* position. Further testing of the *ortho* aniline, (*R*)-**5o**, resulted in an IC_{50} value of 123 nM. All these groups are regarded as weak hydrogen bond acceptors [26], and the activity trend OMe > OH > NH_2 might

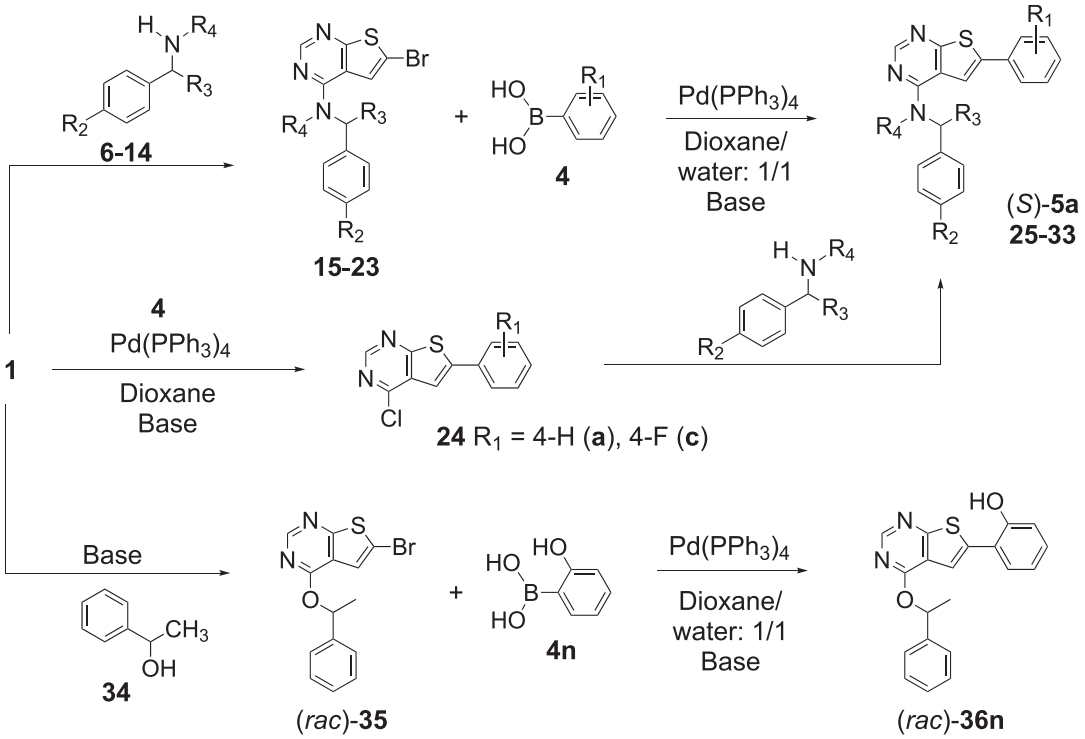

	R_2	R_3	R_4
6, **15**	F	Me	H
7, **16**	H	H	H
8, **17**	H	CH_2CH_3	H
9, **18**	H	$CH(Me)_2$	H
10, **19**	H	Me	Me
11, **20**	H	CF_3	H
12, **21**	H	CH_2F	H
13, **22**	H	CH_2OMe	H
14, **23**	H	CH_2OH	H

	R_1	R_2	R_3	R_4
25a	H	F	Me	H
25c	4-F	F	Me	H
25e	4-CH_2OH	F	Me	H
25j	3-OH	F	Me	H
25l	3-CH_2OH	F	Me	H
25n	2-OH	F	Me	H
25p	2-OMe	F	Me	H
25q	2-CH_2OH	F	Me	H

	R_1	R_2	R_3	R_4
26n	2-OH	H	H	H
27n	2-OH	H	CH_2CH_3	H
28n	2-OH	H	$CH(Me)_2$	H
29n	2-OH	H	Me	Me
30n	2-OH	H	CF_3	H
31n	2-OH	H	CH_2F	H
32n	2-OH	H	CH_2OMe	H
33n	2-OH	H	CH_2OH	H

	R_1	R_2	R_3	R_4
33e	4-CH_2OH	H	CH_2OH	H
33p	2-OMe	H	CH_2OH	H
33s	2-OMe, 4-CHO	H	CH_2OH	H
33t	2-OMe, 4-CH_2OH	H	CH_2OH	H

Scheme 2. Synthesis and structures of the thienopyrimidines (*S*)-**5a**, **25**–**33** and (*rac*)-**36n**.

therefore be due to difference in desolvation energies, leading to the highest potency for the least solvated compound (*R*)-**5p**.

For the hydroxymethyl group the potency increased in the order *ortho* < *meta* < *para*, strongly indicating that a hydrogen donor/acceptor group at this position promotes binding. Possibly, this interaction can be reached also from the *meta* position, explaining the similar activity of (*R*)-**5l** and (*R*)-**5e**.

To investigate the effect of substituent size and possible long range electronic effects on N-1 and N-3, the additional compounds (*R*)-**5g**–**i** were made and tested. The aldehyde derivative (*R*)-**5i**, being small and electron withdrawing had a decent potency (11 nM), whereas the bulky *tert*-butyl and trifluoromethyl compounds having opposite electronic character both were not tolerated in the *para* position. This shows that bulky *para* substituents reduce activity. The ^{13}C NMR spectroscopic shift changes at C-2 and C-4 of compounds (*R*)-**5a**–**r** followed normal substituent effects where electron donating groups increase shielding (see Supporting information). However, no correlation of the ^{13}C chemical shifts with the IC_{50} values was seen. Thus, the data do not indicate that long range electronic effects have any major influence on EGFR inhibitory potency. A low activity was also noticed for the 2,4,6-trisubstituted derivatives, (*R*)-**5u**, **v**.

2.3.2. Structural variations in Fragment B

To clarify the role of the 4-amino group (Fragment B, Fig. 2) in protein-ligand binding, the size and electronic properties of R_3 have been varied and R_4 blocked as methyl. Moreover, modification of R_3 might reveal favourable interactions and size limitations in this

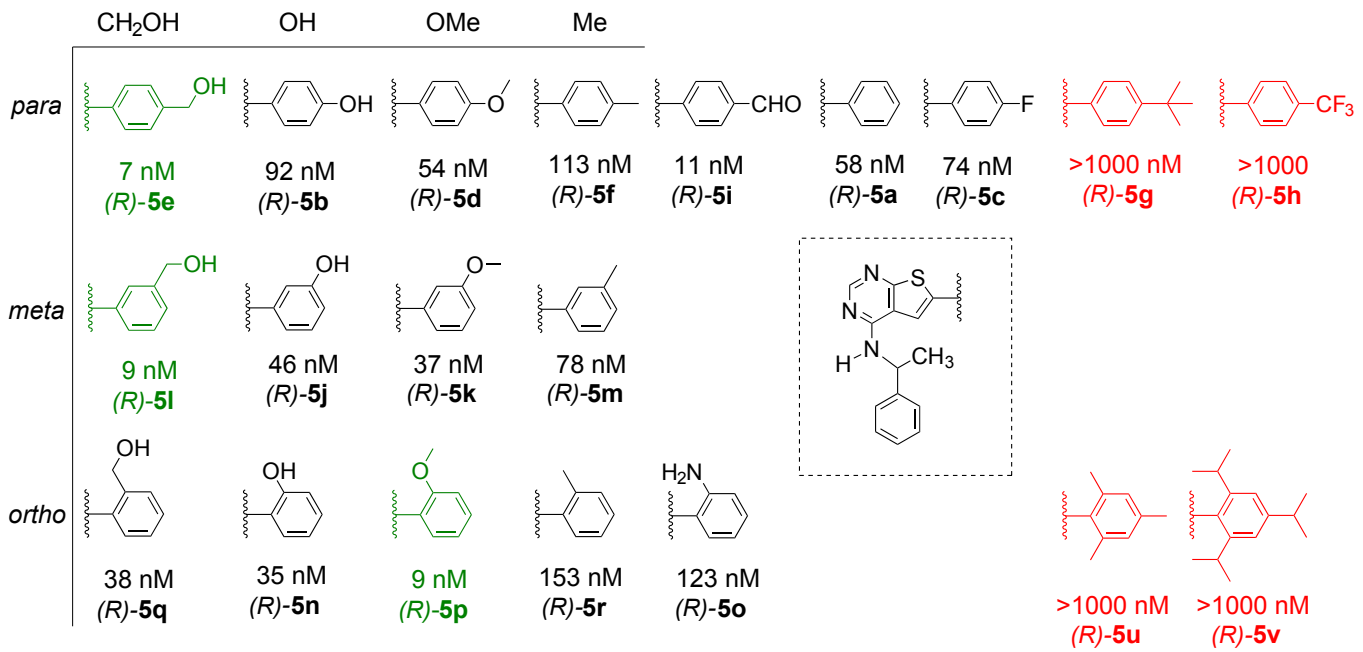

Fig. 4. IC_{50} values of compounds **5a**–**r** and **5u**, **v** towards EGFR-TK. (Single point data and standard deviations of the IC_{50} are compiled in Supporting information).

part of the binding pocket. The results of the testing are summarized in Fig. 6.

Conservative modifications at R_3 as exemplified with the benzylamine based **26n** and 1-phenyl-1-propanamine derivative (*R*)-**27n** had similar activity to that of (*R*)-**5n**. The racemic monofluoro and isopropyl analogues (*rac*)-**31n** and (*rac*)-**28n** showed IC_{50} values of 67 and 55 nM, respectively, indicating that the enantiomerically pure analogues also would have a decent EGFR inhibitory potency. The trifluoromethyl compound (*rac*)-**30n** on the other hand had low activity. As the trifluoromethyl group has a size similar to an isopropyl [27,28], the low potency could be due to the inductive effect reducing amine basicity, although conformational effects cannot be ruled out.

A low activity was also the case when removing the hydrogen donor ability of the 4-amino group by methylation, as in compound (*R*)-**29n**, and when using oxygen as heteroatom (compound (*rac*)-**36n**). This strongly suggests that a secondary 4-amino group is crucial for binding interactions with EGFR-TK.

In the search for hydrogen bonding interactions and strengthened lipophilic contacts the R_3 side chain was also varied with a methoxymethyl and a hydroxymethyl group. To our delight compound (*S*)-**33n** (IC_{50} 3 nM) was found to be 10 times more potent than the reference compound (*R*)-**5n**. A decent activity was also seen for the methylated analogue (*S*)-**32n** (IC_{50} 14 nM). In the late phase of our work we discovered that a related thienopyrimidine, containing the same hydroxylmethyl side chain, has been identified as EGFR reversible inhibitor with an IC_{50} value of 720 nM, which is 36 times less potent than Gefitinib in the assay used [23]. The same group later discovered that the hydroxymethyl side chain is hydrogen bonded to Asp in the Asp-Phe-Gly motif [29].

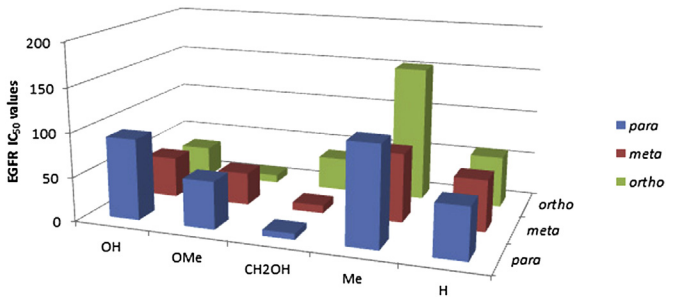

Fig. 5. Effect of 6-aryl substitution pattern on EGFR potency.

Testing of compound (*S*)-**5a** (IC_{50} > 1000) verified that the absolute stereochemistry is of uttermost importance. This was also confirmed in the case of (*S*)-**5n**, (*R*)-**32n** and (*R*)-**33n**. Note that although the relative stereochemistry is the same, the *R*/*S* nomenclature in case of derivatives **32** and **33** changes as a result of the higher priority of the CH_2O– as compared to the phenyl group.

Based on this we conclude that trifluoromethyl as R_3, the hydrogen bond donor ability of the 4-amino group, and wrong stereochemistry affects potency negatively. The steric bulk of the R_3 group is of less importance for potency, while a hot spot interaction can be reached with a hydroxymethyl substituent at the stereocentre.

2.3.3. Fluoro insertion in the aromatic part of Fragment B

Previous work on pyrrolopyrimidines indicated that only limited structural variation was tolerated in the aromatic part of Fragment B [12], however *para*-fluoro substituted analogues showed promising activity. As blocking of metabolic labile sites by introduction of fluoro atoms is an efficient strategy in drug design [30,31], selected *para*-fluoro derivatives were prepared and tested. The obtained EGFR-TK IC_{50} values are compared with those for the corresponding nonfluorinated derivatives in Fig. 7.

The *para*-fluoro substituted derivatives **25** showed consistently lower potency as compared to the non-fluorinated analogues **5**. This systematic trend strongly suggests that all ligands, independent of the 6-aryl substitution pattern, bind in a similar way. The lower activity observed on fluoro insertion did not inspire more elaborate structure–activity studies in this region of the molecule.

2.3.4. Increasing potency by combining active fragments

To investigate if more active compounds could be developed, the favourable substitution patterns identified were combined into new compounds. (*S*)-2-Amino-2-phenylethan-1-ol ((*S*)-**14**) and (*R*)-1-phenylethylamine ((*R*)-**2**) were used as building blocks in Fragment B, while the substructures in Fragment A included 2-

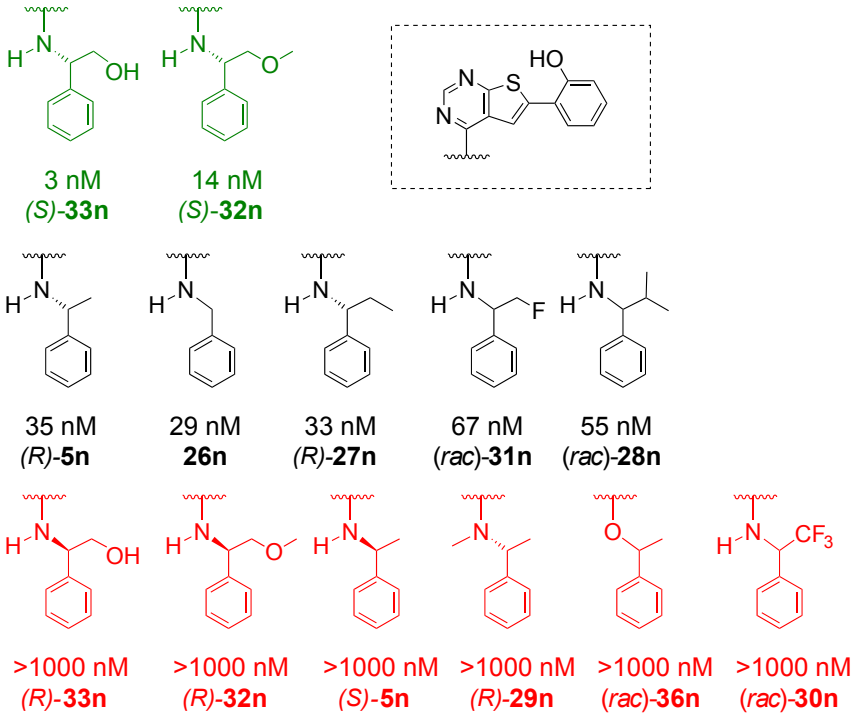

Fig. 6. EGFR inhibitory potency represented by IC_{50} values upon variation of Fragment B. (Single point data and standard deviations of the IC_{50} are compiled in Supporting information).

methoxyphenyl, 4-hydroxymethylphenyl and a combination of these. The compounds made, and the test results in terms of IC_{50} values are shown in Fig. 8.

Three compounds were identified as highly potent (<1 nM), of which the most active, compound (*S*)-**33t**, showed a 200 fold improvement in IC_{50} as compared to the starting point (*R*)-**5a**. Moreover, in every case the combination strategy was successful for improving the potency.

2.3.5. *Structure–activity relationships and molecular modelling*

The major conclusions regarding the identified structure–activity relationships are summarized in Fig. 9.

Also, molecular docking was undertaken using crystal data from a protein co-crystallized with AEE-788 (2J6M) (Fig. 11), which initially indicated several binding modes. Herein, we have assumed that binding should involve the N-1 to Met793 interaction as shown in the co-crystal structure of AEE-788 and EGFR [10].

Upon variations in Fragment B, an increase in EGFR potency was seen when having hydroxymethyl or methyl ether in the R_3 side chain. Modelling indicates these groups to engage in a hydrogen bonding network involving Thr854 and Asp855 in the DFG motif. The same type of interaction has been seen in a related 5,6-diarylfuropyrimidine [29].

Further, a secondary amine function is needed at C-4, as also seen in other classes of EGFR inhibitors [32]. Moreover, the electronic nature of the R_3 substituent, influencing the basicity of this amine, and the stereochemistry are of outmost importance. Overall, this points to the fact that the secondary NH group is involved in

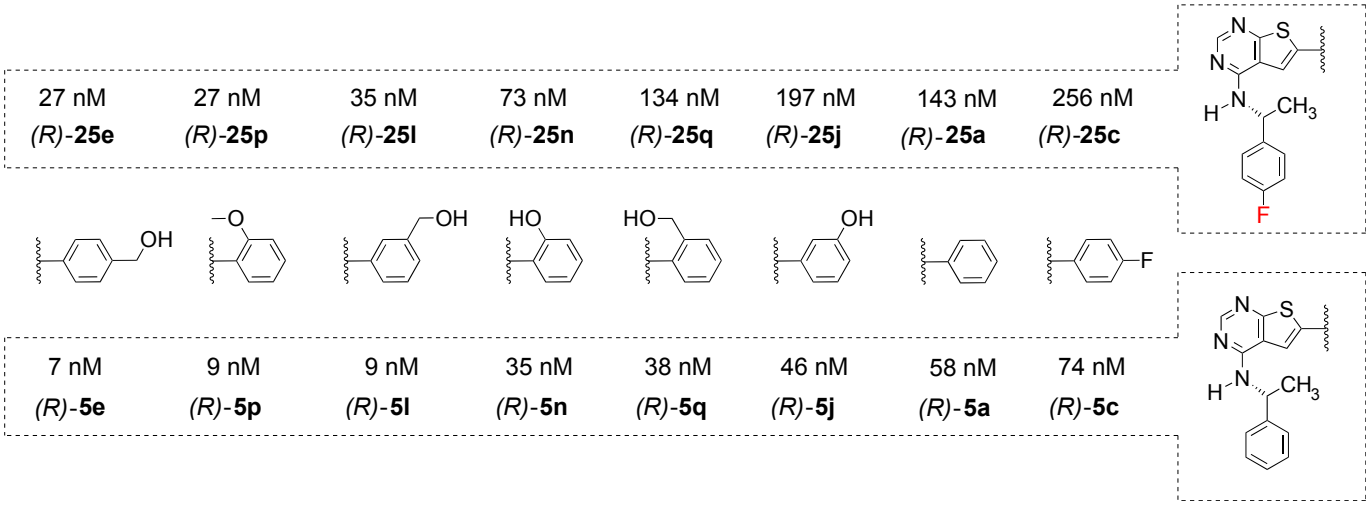

Fig. 7. Comparison of EGFR-TK inhibitory activity for fluorinated and nonfluorinated analogues. (Single point data and standard deviations of the IC_{50} are compiled in Supporting information).

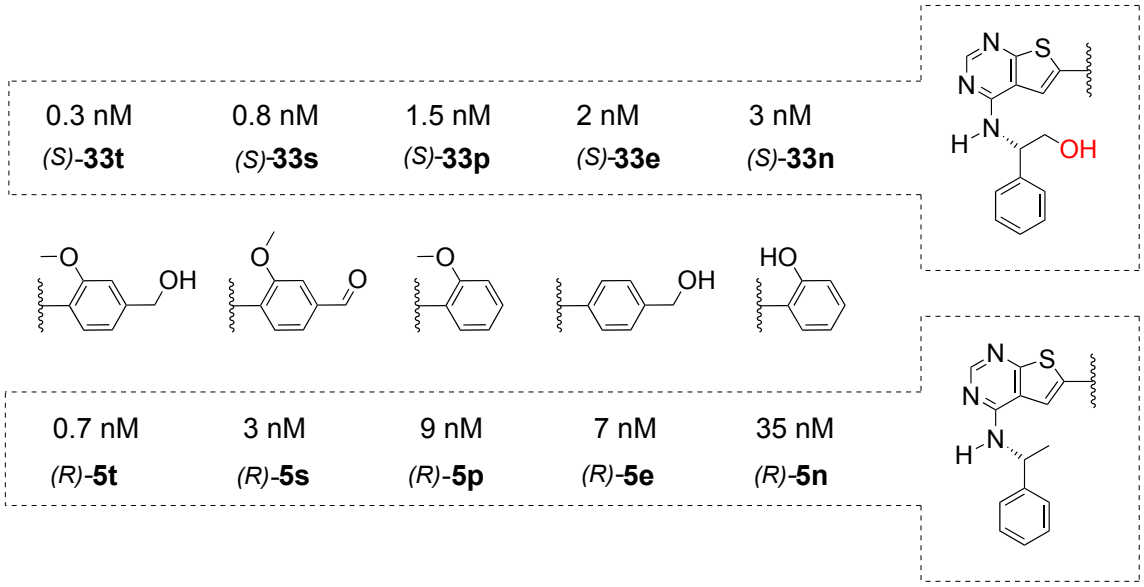

Fig. 8. EGFR-TK inhibitory activity (IC_{50} nM) by combining active fragments. (Single point data and standard deviations of the IC_{50} are compiled in Supporting information).

binding interactions. Two water molecules were seen in close proximity (2.6–2.8 Å) to the C-4 amino group, whereas one of these appears to donate a hydrogen bond to N-3 as seen from Fig. 11. Possibly, the secondary amino group forms part of a hydrogen bonding network involving these water molecules as indicated in the crystallization and modelling work of Park et al. [11].

The naked phenyl ring (Fragment B) is located in a hydrophobic pocket as observed for AEE-788. This model explains the reduced activity of the *para*-fluoro containing derivatives **25** to be due to repulsive interactions between the fluoro substituent and especially Thr790. Other residues in close proximity include Leu777, Leu788 and Ile789. As compared to the analogues pyrrolopyrimidines [12], a higher sensitivity to fluoro insertion was seen. Thus, a slightly distorted binding of the ligands as compared to the pyrrolopyrimidines is indicated.

It was initially speculated that the pyrrole nitrogen could be involved in hydrogen bonding as a donor. This is an interaction which is not satisfied by the thienopyrimidine based molecules. Placing hydrogen bond donor groups as R_1 (OH, NH_2 or CH_2OH) did not have a huge impact on potency, indicating that the intrinsic

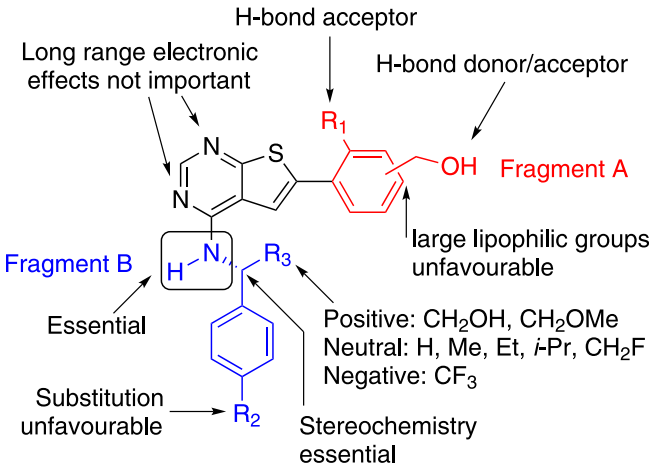

Fig. 9. Structure–activity relationships identified in this study.

higher activity in the pyrrolopyrimidine **III** as compared to (*R*)-**5a**, is due to the slight change in orientation of the 6-aryl ring (Fig. 10).

The 6-aryl group (Fragment A) is directed towards the bulk solvent, and an indication of hydrogen bonding is seen from *para* hydroxymethyl to Leu718. Further, it is postulated that this site also could be reached from the *meta* position with the same group.

Finally, a weak hydrogen bond acceptor (OMe) was preferred in the *ortho* position, and oriented towards NH of Gly796, which might be a hydrogen bond donor, although the O··HN distance was a long as 3.1 Å. Gly796 has previously been postulated to be engaged in a van der Waals interaction with the methoxy group of Gefitinib [3], which offers an alternative explanation of the effect exerted by the methoxy group.

The pyrimidine nitrogens have been proposed as crucial for EGFR ligand binding. The ^{13}C NMR spectroscopic data (Supporting information) indicates that a long range electronic effect from the 6-aryl group does affect the electron density of the pyrimidine. However, in the activity range studied other variables, mainly polar interactions of the side chains seem to be of higher importance.

2.3.6. Further profiling of selected compounds

Compounds (*S*)-**33t**, (*R*)-**5t**, (*S*)-**33p** and Erlotinib, were further evaluated at 10 and 100 nM ATP concentrations towards EGFR-TK,

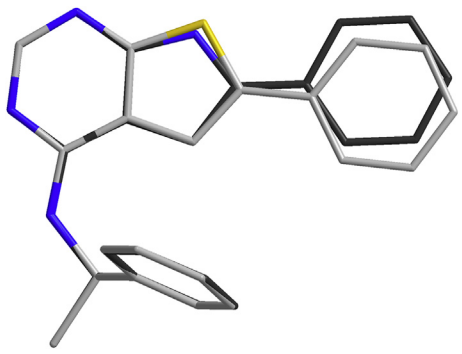

Fig. 10. Overlaid structures of **III** (dark grey) and (*R*)-**5a** (light grey). Replacement of the heteroatom leads to a shift of 0.7 Å of the carbon in *para* position of the 6-aryl ring (Fragment A).

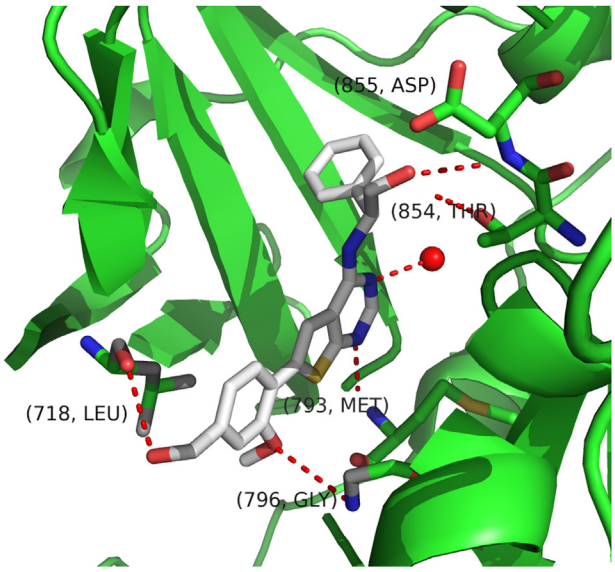

Fig. 11. Docked structure of (*S*)-**33t** in EGFR. Polar interactions and hydrogen bonds towards Leu718, Met793, Thr854 and Gly796 are highlighted.

and the EGFR mutants L858R, L861Q and T790M. The results are shown in Table 1.

As the ATP concentration equal to Km is close to 10 μM, the testing at 10 μM of ATP (Table 1, entry 2) was only useful for verifying the high activity. By increasing the ATP concentration to 100 μM the IC_{50} values were increased, confirming that these are reversible inhibitors. In addition, very similar high potencies were also seen towards the EGFR L858R and L861Q mutants (entries 4, 5). As expected for reversible inhibitors, these compounds were not active in the nanomolar range towards the EGFR T790M mutants

Table 1
Inhibitory potency of (*S*)-**33t**, (*R*)-**5t**, (*S*)-**33p** and Erlotinib towards EGFR at different ATP concentrations and towards the mutants L858R, L861Q and T790M. Unless otherwise stated reported IC_{50} values are the mean of two titration curves (a total of 20 data points).

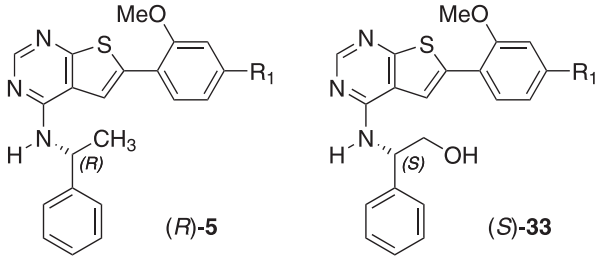

R_1 = H (**p**), CH_2OH (**t**)

Entry	Kinase	ATP conc.	Erlotinib	(*S*)-**33t**	(*R*)-**5t**	(*S*)-**33p**
1	IC_{50} (nM) EGFR ($n = 6$)[a]	Km app	0.4 ± 0.1	0.3 ± 0.1	0.7 ± 0.2	1.5 ± 1.0
2	IC_{50} (nM) EGFR ($n = 2$)	10 μM	0.3 ± 0.0	0.4 ± 0.0	0.6 ± 0.1	2.6 ± 0.6
3	IC_{50} (nM) EGFR ($n = 2$)	100 μM	1.7 ± 0.1	1.0 ± 0.0	2.0 ± 0.3	10.2 ± 0.1
4	IC_{50} (nM) EGFR-L858R ($n = 2$)	Km app	0.6 ± 0.1	0.3 ± 0.1	1.0 ± 0.1	1.3 ± 0.2
5	IC_{50} (nM) EGFR-L861Q ($n = 2$)	Km app	0.5 ± 0.0	0.3 ± 0.0	0.8 ± 0.1	1.0 ± 0.5

[a] Reported IC_{50} values are the mean of six titration curves (a total of 60 data points).

(data not shown) [3]. Overall, compound (*S*)-**33t** compares favourably with Erlotinib.

Off-target activity is often a challenge in development of kinase inhibitors. The selectivity of compounds (*S*)-**33t** and (*R*)-**5t** as kinase inhibitors were therefore evaluated towards a panel of 47 other kinases at a test concentration of 500 nM, see Table 2.

Compounds (*R*)-**5t** and (*S*)-**33t** have very similar structures, and this is also reflected in the selectivity screen. For the majority of the 48 kinases tested, the two compounds have approximately the same potency. The selectivity profiles of the two compounds are compared with that of Erlotinib by a Gini plot (Fig. 12), where the cumulative fraction of kinases are plotted towards the cumulative fraction of total inhibition [33].

As seen (*S*)-**33t** (Gini coefficient: 0.60) and Erlotinib (Gini coefficient: 0.58) have comparable kinase selectivity profile, whereas compound (*R*)-**5t** (Gini coefficient: 0.68) is a somewhat more selective EGFR kinase inhibitor.

Although a low activity was seen towards most of the kinases, a mediocre inhibition efficiency was observed towards HER2, and the kinases LYN A and LYN B. Whereas HER2 is directly involved in EGFR signalling as a dimerization partner, the LYN kinases are overexpressed in myelodysplastic syndrome and leukaemia [34–36], and also affect EGFRvIII activity [37]. Thus, their inhibition in cancerous diseases might be beneficial [36,37]. The inhibition of some kinases like Aurora kinases, BRAF, PLK's, PDGER's, VEGFR's, KIT, ABL, JAK2, PTK2 (FAK) and PIM have been indicated as risk factors for cardiac toxicity [38]. Compounds (*R*)-**5t** and (*S*)-**33t** showed a moderate 22% and 20% inhibition of ABL1 and BRAF at 500 nM test concentration, whereas the others of this selection of kinases showed inhibition of less than 9%.

Table 2
Inhibition of various kinases of compound (*S*)-**33t** and (*R*)-**5t** (500 nM), mean % of two measurements with [ATP] = *K*m.

Kinase	Inhibition (%)		Kinase	Inhibition (%)	
	(*S*)-**33t**	(*R*)-**5t**		(*S*)-**33t**	(*R*)-**5t**
ABL1	22	7	LCK	6	11
AURKA (Aurora A)	5	<1	LYN A	40	61
AURKB (Aurora B)	10	<1	LYN B	56	57
BRAF[a]	20	1	MAP2K1 (MEK1)[a]	18	4
CHEK1 (CHK1)	15	<1	MAPK1 (ERK2)	7	<1
CFS1R (FMS)	3	2	MAPK14 (p38 alpha)	13	<1[a]
CSK	5	7	MAPK8 (JNK1)[a]	14	2
EGFR (ErbB1)	100	98	MAPKAPK2	8	<1
EPHA1	<1	<1	MET (cMet)	3	15
EPHB1	4	<1	NEK1	13	<1
ERBB2 (HER2)	50	57	PDGFRA (PDGFR alpha)	<1	<1
ERBB4 (HER4)	63	30	PDGFRB (PDGFR beta)	<1	3
FER	8	10	PIM2	1	<1
FGFR1	4	<1	PLK1	<1	<1
FGR	58	40	PRKACA (PKA)	nd[b]	2
FLT1 (VEGFR1)	<1	4	PRKCB1 (PKC beta I)	4	<1
FLT4 (VEGFR3)	<1	3	PRKCQ (PKC theta)	<1	<1
FYN	12	<1	PTK2 (FAK)	<1	6
GSK3B (GSK3 beta)	8	7	RET	9	5
HCK	20	5	SRC	9	10
IKBKB (IKK beta)	1	10	STK22B (TSSK2)	8	8
JAK2	9	7	SYK	10	8
KDR (VEGFR2)	12	12	TEK (Tie2)	13	<1
KIT	<1	7	YES1	37	12

[a] [ATP] = 100 μM.
[b] Not determined.

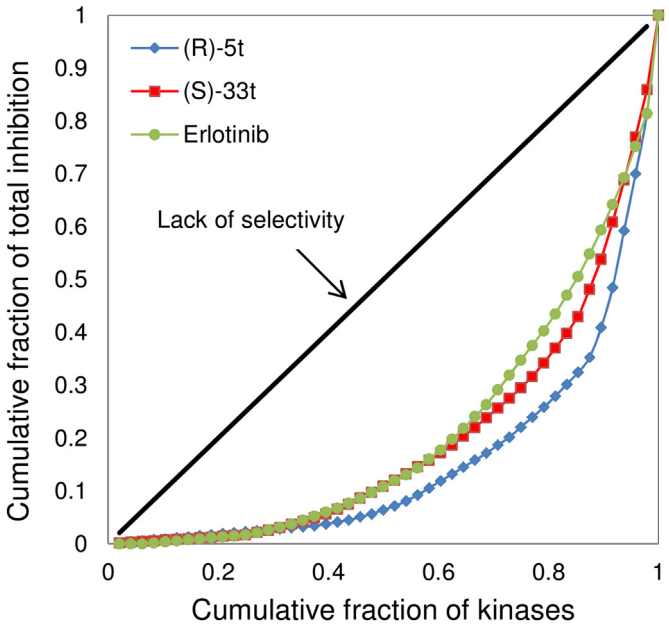

Fig. 12. Gini plot for comparing kinase selectivity of compounds (*R*)-**5t**, (*S*)-**33t** and Erlotinib. The solid line represents a non-selective compound.

The IC_{50} values were used to estimate the relative druglike properties of the candidate inhibitors [39–43], see Table 3. Ligand efficacy (LE) and binding efficiency (BEI) are measures of binding efficiency per heavy atom and molecular weight, respectively. The LE and BEI numbers should be as high as possible. Surface efficiency index (SEI) describes how dependent activity is of polar interactions. A SEI value of 18 has been suggested as a guideline value for good oral bioavailability. Lipophilic ligand efficiency (LLE) describes how dependent binding is of lipophilicity and values in the range of 5–7 are preferable. Lipophilicity corrected ligand efficiency (LELP), is derived from calculated log *P*, and LELP values below 10 has been suggested as optimal.

The binding efficiency as measured pr. heavy atom (LE) or by molecular weight (BEI) of (*S*)-**33t**, (*R*)-**5t** and (*S*)-**33p** are comparable to that of Erlotinib. The surface efficiency index (SEI) is a measure of activity per polar surface area. The suboptimal SEI value of (*S*)-**33t** indicate that the compound might be too polar. On the other hand the hydrophilic/lipophilic balance of (*S*)-**33t** as defined by LLE and LELP indicate favourable properties as compared to Erlotinib. Compounds (*R*)-**5t** and (*S*)-**33p** are suggested to be too lipophilic.

To reveal if the new lead compounds (*S*)-**33t** and (*R*)-**5t** also had on-target cellular potency towards EGFR mutants, they were compared with Erlotinib using a Ba/F3 EGFR-L858R and Ba/F3 EGFR-T790M reporter cells [44]. These systems consist of a murine bone marrow-derived cell line which is dependent on the growth factor interleukin-3 (IL-3), but is rendered IL-3 independent by stable expression of different tyrosine kinase oncogenes. Upon expression of activated EGFR mutant proteins the Ba/F3 cells display growth and survival independent of IL-3, but dependent on the constitutive EGFR signal. Using a Ba/F3 EGFR cellular system, novel inhibitors can be tested for potency against EGFR induced cell growth. On target cellular EGFR activity can thus be confirmed by comparing survival in Ba/F3 cells expressing other activated kinases.

Table 3
Estimated LE, BEI, SEI, LLE and LELP for (*R*)-**5t**, (*S*)-**33p** (*S*)-**33t** and Erlotinib based on IC_{50} values (For details of calculation see Supporting information).

Parameter	Ref. value	(*S*)-**33t**	(*R*)-**5t**	(*S*)-**33p**	Erlotinib
IC_{50} (nM)		0.3	0.7	1.5	0.4
MW (Da)	200–500	407.5	391.5	377.5	393.4
clog *P*[a]	2–5	3.5	4.5	4.2	4.0
PSA[b]		87.5	67.3	67.3	74.7
LE	0.36	0.33	0.33	0.33	0.32
BEI	27	23.4	23.4	23.4	23.9
SEI	18	10.9	13.6	13.1	12.6
LLE	5–7	6.0	4.7	4.7	5.4
LELP	<10	10.8	13.8	12.8	12.3

[a] Calculated log *P*.
[b] Calculated polar surface area (Å^2).

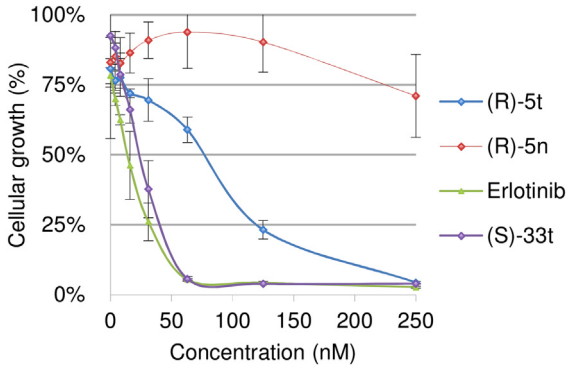

Fig. 13. Effect of (*S*)-**33t**, (*R*)-**5t**, (*R*)-**5n** and Erlotinib on Ba/F3 EGFR-L858R cellular growth.

The Ba/F3 proliferation study was done using the 3-(4,5-dimethylthiazol-2-yl)-2,5-diphenyltetrazolium bromide-assay (MTT). Compounds (*S*)-**33t** and (*R*)-**5t** inhibited Ba/F3 EGFR-L858R in a dose dependent manner in the nanomolar range, see Fig. 13. The Ba/F3 experiments reflected trends from the enzymatic IC_{50} values. Derivative (*S*)-**33t** (IC_{50} 26 nM) was almost equipotent to Erlotinib (IC_{50} 22 nM), while (*R*)-**5t** (IC_{50} 97 nM) was less potent. The *ortho* hydroxy analogue (*R*)-**5n**, included as a reference for an intermediate potent EGFR inhibitor, showed considerably less activity. None of the compounds affected proliferation of the Ba/F3 EGFR-T790M cells (data not shown). Thus, this shows that the tested compounds affect cell proliferation mainly by interfering with the EGFR function.

Further testing of (*S*)-**33t** and Erlotinib was performed with A-431 cells. These cells express abnormally high levels of EGFR [45,46], and contains no functional tumour suppressor protein TP53 [47]. As in the Ba/F3 EGFR-L858R cell system, Erlotinib was more potent than (*S*)-**33t**, with IC_{50} values of 0.4 μM and 1.1 μM, respectively (Table 4). Finally, the compounds were evaluated using human cancer cell lines with different oncogenic profiles, Table 4.

EGFR has been implicated as important for cell signalling in cervical cancers [48]. However, C-33A, a cervix carcinoma cell line, has low EGFR expression [49–52], and no inhibition in cell growth was previously detected using Cetuximab [52]. C-33A was therefore regarded as a challenging cell model. Interestingly, Erlotinib and (*S*)-**33t** both inhibited cell viability with IC_{50} of 0.9 μM and 1.6 μM, respectively. This could indicate that targets other than EGFR are of importance in the inhibitory action of both Erlotinib and (*S*)-**33t**.

Table 4
Cell proliferation study using human cancer cell lines.[a]

Cell line	EGFR profile	Erlotinib IC_{50} (μM)	(*S*)-**33t** IC_{50} (μM)	(*R*)-**5t** IC_{50} (μM)
A-431	High EGFR	0.4 ± 0.0	1.1 ± 0.3	Nd[b]
C-33A	Low EGFR	0.9 ± 0.0	1.6 ± 0.1	4.3 ± 0.8
CAL-27	EGFR	1.3 ± 0.6	2.8 ± 1.4	5.2 ± 1.0
FaDu	EGFR	18 ± 6	43 ± 6	Nd[b]
AU-565	Low EGFR	3.3 ± 0.6	6.3 ± 0.4	15 ± 1
NCI-H82	Low EGFR	>20	10.9 ± 0.2	>20

[a] The data points are shown in Supporting information.
[b] Not determined.

The head and neck cell lines CAL-27 (tongue carcinoma) and FaDu (hypopharnyx carcinoma) also contain multiple genetic defects [53]. These cells were selected as they are known to possess EGFR activity [54,55] and also respond to Erlotinib [56]. In our assay, CAL-27 was considerable more sensitive towards the inhibitors than the FaDu cells, and in both cases Erlotinib showed stronger inhibition of cell proliferation than (*S*)-**33t**.

AU-565, a breast adenocarcinoma cell line has overexpressed HER2, HER3, HER4, and are classified as EGFR negative [57–59]. Although the compounds tested have a decent HER2 and HER4 inhibitory activity in the enzymatic profiling, the cellular IC_{50} values obtained were only mediocre (3.3–15 μM). This indicates that even higher pan-HER inhibitory profile is needed to effectively block cell growth in this system.

NCI-H82, a small cell lung carcinoma cell line, contains multiple oncogens [60,61], and also possesses low level of EGFR and HER2 [62,62], however some potency towards Gefitinib has been observed [62]. Unfortunately, neither of the compounds tested had any considerable activity towards the NCI-H82 cell line.

Overall, the cellular potency of the developed EGFR inhibitor, (*S*)-**33t**, is generally lower than Erlotinib. Based on the comparable EGFR enzymatic inhibitory profile, and the Ba/F3 EGFR-L858R cell model assay, this is most likely due to other cytotoxic effects caused by Erlotinib, rather than differences in druglike properties.

3. Conclusion

A series of 4-*N*-substituted 6-aryl-thienopyrimidines synthesized using Suzuki coupling as the key step, have been evaluated and optimized as EGFR-TK inhibitors.

A stepwise development by combination of favourable substitution patterns led to the discovery of three structures with EGFR $IC_{50} < 1$ nM. The most potent drug candidate identified was equipotent to Erlotinib in enzymatic inhibition studies. Testing towards a panel of kinases revealed a selectivity profile similar to Erlotinib with moderate activity towards HER2, HER4, FGR and LYN A and B kinases. Experiments using a Ba/F3 EGFR-L858R reporter cell-system and human cancer cell lines showed that the candidate compounds had promising cell potency.

The structure–activity relationships study showed that the potency was dependent on the substitution pattern in the 6-aryl group (Fragment A). The activity increased when having a hydroxymethyl substituent in *para* or *meta* position or when placing a methoxy group in the *ortho* position. Both experimental data and modelling indicate that these are polar directional interactions. On the other side a drastic negative effect on potency was seen on introduction of lipophilic and bulky groups in the *para* position. For Fragment B, compounds containing the secondary amine function derived from (*R*)-configured 1-phenylethylamine, 1-phenylpropylamine and benzylamine were all potent inhibitors. Even more active inhibitors were derived from (*S*)-configured 2-amino-2-phenylethan-1-ol. In contrast, using the opposite enantiomers, or when less basic groups were introduced at the stereocentre, a drastic drop in activity was seen. The importance of the secondary amine function was further proved by the low potency of selected model compounds. No evidence suggests that long range electronic effects, originating from the 6-aryl ring, influence potency.

4. Experimental

4.1. General

Compounds (*S*)- and (*R*)-1-phenylethanamine ((*S*)-**2**, (*R*)-**2**), benzylamine (**7**), (*R*)-1-(phenyl)-1-propanamine ((*R*)-**8**), (*R*)-*N*-methyl-1-phenylethan-1-amine ((*R*)-**10**), (*R*)-2-methoxy-1-phenylethan-1-amine ((*R*)-**13**), (*S*)- and (*R*)-2-amino-2-phenylethan-1-ol ((*S*)-**14**, (*R*)-**14**), K_2CO_3, trifluoroacetophenone, acetophenone, 2-methyl-1-phenylpropan-1-one, $NaBH_4$, $NaBH_3CN$, NaH, $Pd(PPh_3)_4$, $Pd(OAc)_2$, $Pd_2(dba)_3$, 2-dicyclohexylphosphino-2′,6′-dimethoxybiphenyl (SPhos) and the arylboronic acids, were from Sigma Aldrich. (2-Hydroxyphenyl)boronic acid (**4n**) and (*R*)-1-(4-fluorophenyl)ethanamine ((*R*)-**6**) were from Alfa Aesar. (4-Formyl-2-methoxyphenyl) boronic acid (**4s**) was from Combi-Blocks. Compound **1** [25], 2-fluoro-1-phenylethan-1-amine (*rac*-**12**) [63], were prepared as described previously, while 4-chloro-6-phenylthieno[2,3-*d*]pyrimidine (**24a**) [25], (*rac*)-**35** and (*rac*)-**36n** [64], were prepared and characterised in other studies from our laboratory.

Silica-gel column chromatography was performed using silica gel 60A from Fluka, pore size 40–63 μm. Celite 545 from Fluka was also used.

4.2. Analyses

^1H and ^{13}C NMR spectra were recorded with Bruker Avance 400 spectrometer operating at 400 MHz and 100 MHz, respectively. ^{19}F NMR was performed on a Bruker Avance 500 operating at 564 MHz. For ^1H and ^{13}C NMR chemical shifts are in ppm rel. to TMS or DMSO-d_6, while for ^{19}F NMR the shift values are relative to hexafluorobenzene. Compounds isolated as their HCl salts were free-based prior to NMR spectroscopic analysis. Coupling constants are in hertz. HPLC (Agilent 110-Series) with a G1379A degasser, G1311A Quatpump, G1313A ALS autosampler and a G1315D Agilent detector (254 nm) was used to determine the purity of the synthesised compounds. All compounds evaluated for EGFR inhibitory potency had a purity of ≥95%. Conditions: Method A: Poroshell C18 (100 × 4.6 mm) column, flow rate 0.8 mL/min, elution starting with water/CH_3CN (90/10), 5 min isocratic elution, then linear gradient elution for 35 min ending at CH_3CN/water (100/0). Method B: Poroshell C18 (100 × 4.6 mm) column, flow rate 1.0 mL/min, elution starting with water + 0.1% TFA/CH_3CN (95/5), linear gradient elution for 25 min ending at CH_3CN/water + 0.1% TFA (100/0), then 20 min isocratic elution. Method C: Poroshell C18 (100 × 4.6 mm) column, flow rate 1.0 mL/min, elution starting with water + 0.1% TFA/CH_3CN (98/2), linear gradient elution for 25 min ending at CH_3CN/water + 0.1% TFA (90/10), then 20 min isocratic elution. The software used with the HPLC was Agilent ChemStation. Chiral HPLC was conducted on a Lux 5u Cellulose-1 4.6 × 250 mm chiral column (part no. 00G-4459-E0). Eluting with hexane (cont. 0.2% diethyl amine)/*i*-PrOH, 96/4, flow rate: 2 mL/min, detection at 254 nm. The retention times were: (*R*)-**5**: 5.7 min and (*S*)-**5**: 7.8 min, both with 99% ee.

Accurate mass determination (ESI) was performed on an Agilent G1969 TOF MS instrument equipped with a dual electrospray ion source, or EI (70 eV) using a Finnigan MAT 95 XL. Accurate mass determination in positive and negative mode was performed on a "Synapt G2-S" Q-TOF instrument from Waters. Samples were ionized by the use of an ASAP probe, no chromatography separation was used before the mass analysis. FTIR spectra were recorded on a Thermo Nicolet Avatar 330 infrared spectrophotometer. All melting points are uncorrected and measured by a Stuart automatic melting point SMP40 apparatus.

4.3. Synthesis of primary amines

4.3.1. (rac)-2-Methyl-1-phenylpropan-1-amine ((rac)-9) [65]

2-Methyl-1-phenylpropan-1-one (3.05 g, 20.6 mmol) was mixed with ammonium acetate (15.8 g, 206 mmol) in dry MeOH (50 mL). Sodium cyanoborohydride (1.31 g, 20.6 mmol) was added, and the reaction was stirred at 50 °C for 18 h. After cooling to rt, the reaction mixture was concentrated *in vacuo* and CH_2Cl_2 (50 mL)

was added. The mixture was washed with water (3 × 50 mL), and the water phases were back extracted with CH_2Cl_2 (2 × 50 mL). The combined organic phases were washed with saturated aq $NaHCO_3$ solution (50 mL), dried over anhydrous Na_2SO_4, filtrated and concentrated. This gave 3.96 g (18.9 mmol, 92%) of (*rac*)-**9** as a clear oil. ^{1}H NMR (300 MHz, $CDCl_3$) δ: 7.33–7.20 (m, 5H), 3.58 (d, J = 7.3, 1H), 1.90–1.79 (m, 1H), 1.57 (br s, 2H), 0.97 (d, J = 6.7, 3H), 0.76 (d, J = 6.8, 3H). The shifts were ca 0.04 ppm up-field shifted as compared to that reported [65].

4.3.2. (rac)-2,2,2-Trifluoro-1-phenylethanamine ((rac)-**11**) [66]

Compound **11** was made in two steps as reported previously by Scopes et al. [66]. Trifluoroacetophenone (30.0 g, 172 mmol), hydrochloric hydroxylamine (23.9 g, 344 mmol) and sodium acetate (32.5 g, 396 mmol) were dissolved in water (100 mL) and EtOH (50 mL). The mixture was heated to 75 °C and stirred for 24 h. EtOH was removed *in vacuo* and the mixture was left standing at 4 °C for 72 h. The precipitate formed was isolated by filtration, washed with cold water (3 × 50 mL) and dried under reduced pressure to give 30.7 g (162 mmol, 94%) of 2,2,2-trifluoro-1-phenylethanone oxime as white crystals, mp 62–64 °C; ^{1}H NMR (300 MHz, $CDCl_3$) δ: 8.48 (br s, 1H), 7.53–7.44 (m, 5H). 2,2,2-Trifluoro-1-phenylethanone oxime (30.0 g, 159 mmol) was mixed with Pd/C (10%, 1.13 g) in THF (200 mL) and acetic acid (11.4 g, 10.9 mL, 190 mmol). In a closed reactor the mixture was flushed with hydrogen at 5.5 bar for 23 h, filtered over celite and washed with CH_2Cl_2 (200 mL). The solvent was removed *in vacuo* and 5 M HCl was added to reach pH = 1. The mixture was extracted with diethyl ether (3 × 80 mL). The water phase was added sodium hydroxide until the solution reached pH = 14. Extraction with diethyl ether (3 × 80 mL), removal of the solvent *in vacuo* and distillation (50 mbar, 77 °C) gave 20.6 g (117.3 mmol, 74%) of (*rac*)-**11** as a colourless liquid. ^{1}H NMR (300 MHz, $CDCl_3$) δ: 7.35–7.28 (m, 5H), 4.28 (q, J = 7.4, 1H), 1.68 (br s, 2H). ^{1}H NMR corresponds well with that reported previously at 500 MHz [67].

4.3.3. (S)-2-Methoxy-1-phenylethan-1-amine ((S)-**13**) [68]

Sodium hydride (700 mg, 29.2 mmol) was dissolved in dry THF (10 mL) under an N_2 atmosphere. Then adding (*S*)-2-amino-2-phenylethan-1-ol ((*S*)-**14**) (2.21 g, 14.58 mmol) dissolved in dry THF (20 mL) was added drop wise and stirred for 1 h. The solution was cooled to 0 °C before 2 M MeI in *tert*-butyl methyl ether (7.7 mL, 15.4 mmol) was added drop wise over 30 min using a syringe pump. The reaction was heated at reflux for 3 h. Then the mixture was cooled to rt, diluted with water (50 mL) and diethyl ether (150 mL). After phase separation, the water phase was extracted with more diethyl ether (2 × 60 mL). The combined organic phases were washed with saturated aq NaCl solution (50 mL), dried over anhydrous Na_2SO_4, filtered and concentrated. The crude product was purified by silica-gel column chromatography (CH_2Cl_2/MeOH, 19/1), R_f = 0.59. Isolation and drying gave 1.79 g (11.8 mmol, 81%) of (*S*)-**13** as a colourless oil. ^{1}H NMR (300 MHz, $CDCl_3$) δ: 7.41–7.25 (m, 5H), 4.21 (dd_{AB}, J = 8.8, 3.8, 1H), 3.51 (dd_{AB}, J = 8.7, 3.9, 1H), 3.32–3.39 (m, 4H), 1.74 (s, 2H). The ^{1}H NMR spectroscopic shifts correspond to that reported [68].

4.4. Synthesis of 6-bromo-thieno[2,3-d]pyrimidin-4-amines

4.4.1. General procedure for thermal amination of 4-chloro-thieno[2,3-d]pyrimidins

Compound **1** (1.00 g, 4.01 mmol) was mixed with the benzylamine (12.03 mmol) and 1-butanol (3.5 mL) and agitated at 145 °C for 18–24 h. Then the mixture was cooled to rt, diluted with water (50 mL) and diethyl ether (150 mL) or EtOAc (150 mL). After phase separation, the water phase was extracted with more diethyl ether (2 × 50 mL) or EtOAc (2 × 50 mL). The combined organic phases were washed with saturated aq NaCl solution (50 mL), dried over anhydrous Na_2SO_4, filtered and concentrated *in vacuo*, before the crude oil was dried under reduced pressure to constant weight to remove excess benzylamine. The compounds were purified by silica-gel column chromatography or crystallized as specified for each individual compound.

4.4.2. (R)-6-Bromo-N-(1-phenylethyl)thieno[2,3-d]pyrimidin-4-amine hydrochloride ((R)-**3** HCl) [25]

Compound **1** (5.00 g, 20.04 mmol) was mixed with (*R*)-1-phenylethanamine ((*R*)-**2**) (7.7 mL, 0.60 mol) and 1-butanol (16.5 mL) and agitated at 145 °C for 18 h. Then the mixture was cooled to rt, diluted with water (300 mL) and diethyl ether (300 mL). After phase separation, the water phase was extracted with more diethyl ether (2 × 150 mL). The combined organic phases were washed with saturated aq NaCl solution (150 mL), dried over anhydrous Na_2SO_4, filtered and concentrated *in vacuo*, before the crude oil was dried under reduced pressure to constant weight to remove excess amine. The product was dissolved in diethyl ether (150 mL) and precipitated upon addition of HCl in diethyl ether (8 mL). The solid formed was isolated by filtration and washed with diethyl ether (2 × 100 mL). Drying gave 6.89 g (18.6 mmol, 94%) of (*R*)-**3**·HCl as a white solid, mp 186–195 °C; HPLC purity: 99% (method A), t_R = 27.3 min; $[\alpha]_D^{20}$ = −182.0 (*c* 0.70, DMSO); ^{1}H NMR (400 MHz, DMSO-d_6) δ: 8.27 (s, 1H), 8.23 (d, J = 7.8, 1H), 7.99 (s, 1H), 7.42–7.37 (m, 2H), 7.34–7.28 (m, 2H), 7.24–7.19 (m, 1H), 5.51–5.42 (m, 1H), 1.53 (d, J = 7.0, 3H). The spectroscopic properties corresponds well with that reported previously [25].

4.4.3. (S)-6-Bromo-N-(1-phenylethyl)thieno[2,3-d]pyrimidin-4-amine ((S)-**3**)

The synthesis was performed as described in Section 4.4.1 starting with compound **1** (501 mg, 2.01 mmol) and (*S*)-1-phenylethanamine ((*S*)-**2**) (730 mg, 6.03 mmol). The reaction time was 19 h. The crude product was purified by silica-gel column chromatography (EtOAc/*n*-pentane, 4/1), R_f = 0.69. Isolation and drying gave 545 mg (1.64 mmol, 81%) of (*S*)-**3** as a white solid, mp 121–124 °C; HPLC purity: 98% (method A), t_R = 28.5 min; $[\alpha]_D^{20}$ = 205.1 (*c* 0.55, DMSO); ^{1}H NMR (400 MHz, DMSO-d_6) δ: 8.26 (s, 1H), 8.23 (d, J = 7.7, 1H), 7.99 (s, 1H), 7.41–7.38 (m, 2H), 7.36–7.28 (m, 2H), 7.23–7.19 (m, 1H), 5.51–5.42 (m, 1H), 1.53 (d, J = 7.1, 3H); HRMS (APCI/ASAP, *m*/*z*): 334.0009 (calcd. $C_{14}H_{13}^{79}BrN_3S$, 334.0014, $[M + H]^+$).

4.4.4. (R)-6-Bromo-N-(1-(4-fluorophenyl)ethyl)thieno[2,3-d]pyrimidin-4-amine hydrochloride ((R)-**15**·HCl)

The synthesis was performed as described in Section 4.4.1 starting with compound **1** (1.50 g, 6.00 mmol) and (*R*)-1-(4-fluorophenyl)-ethylamine ((*R*)-**6**) (2.66 g, 19.2 mmol). The reaction time was 24 h. The product was purified by silica-gel column chromatography (EtOAc), R_f = 0.67. The product was precipitated by dissolving in diethyl ether (30 mL), and then addition of HCl in diethyl ether (0.5 mL) followed by crystallization at 4 °C for 2 h. The solid was isolated by filtration. This gave 2.06 g (5.30 mmol, 89%) of (*R*)-**15**·HCl as a white solid, mp 127–129 °C; HPLC purity: 99% (method C), t_R = 18.2 min; $[\alpha]_D^{20}$ = −200.3 (*c* 1.01, DMSO); ^{1}H NMR (400 MHz, DMSO-d_6) δ: 8.27 (s, 1H), 8.23 (d, J = 7.9, 1H), 7.97 (s, 1H), 7.46–7.40 (m, 2H), 7.17–7.10 (m, 2H), 5.50–5.40 (m, 1H), 1.52 (d, J = 7.1, 3H); ^{13}C NMR (100 MHz, DMSO-d_6) δ: 166.5, 162.2 (d, J = 240.7), 154.7, 154.1, 140.6 (d, J = 3.0), 128.0 (d, J = 8.0, 2C), 122.8, 116.8, 115.1 (d, J = 21.1, 2C), 109.7, 48.5, 22.5; ^{19}F NMR (564 MHz, DMSO-d_6) δ: −118.6 (s); IR (neat, cm^{-1}): 3222, 3026, 2358, 1600, 1501, 790, 555; HRMS (EI, 70 eV, *m*/*z*): 350.9835 (calcd. $C_{14}H_{11}N_3^{79}BrFS$, 350.9836, $[M]^+$).

4.4.5. *N*-Benzyl-6-bromothieno[2,3-d]pyrimidin-4-amine (**16**)

The synthesis was performed as described in Section 4.4.1 starting with compound **1** (1.00 g, 4.01 mmol) and benzylamine (**7**) (1.30 mL, 1.28 g, 11.9 mmol). The reaction time was 19 h. Workup and drying gave 1.19 g (3.33 mmol, 83%) of **16** as a light yellow solid, mp 188–190 °C; HPLC purity: 99% (method B), t_R = 15.1 min; ^{1}H NMR (400 MHz, DMSO-d_6) δ: 8.51 (t, J = 5.9, 1H), 8.33 (s, 1H), 7.85 (s, 1H), 7.37–7.29 (m, 4H), 7.27–7.21 (m, 1H), 4.73 (d, J = 5.9, 2H); ^{13}C NMR (100 MHz, DMSO-d_6) δ: 166.5, 155.6, 154.2, 139.1, 128.4 (2C), 127.3 (2C), 126.9, 122.6, 116.9, 109.7, 43.3; IR (neat, cm^{-1}): 3235, 3024, 2922, 1594, 1448, 1309, 1084, 848, 774, 746, 694; HRMS (ESI, m/z): 319.9851 (calcd. $C_{13}H_{11}^{79}BrN_3S$, 319.9852, $[M + H]^+$).

4.4.6. (*R*)-6-Bromo-*N*-(1-phenylpropyl)thieno[2,3-d]pyrimidin-4-amine ((*R*)-**17**)

The synthesis was performed as described in Section 4.4.1 starting with compound **1** (200 mg, 0.80 mmol) and (*R*)-1-phenylpropan-1-amine ((*R*)-**8**) (329 mg, 2.43 mmol). The reaction time was 20 h. The crude product was absorbed onto silica and purified by silica-gel column chromatography (*n*-pentane/EtOAc, 4/1), R_f = 0.35. Drying gave 205 mg (0.53 mmol, 67%) of (*R*)-**17** as a white solid, mp 142–147 °C; HPLC purity: 99% (method B), t_R = 18.2 min; $[\alpha]_D^{20}$ = −166.8 (*c* 0.98, DMSO); ^{1}H NMR (400 MHz, DMSO-d_6) δ: 8.26 (s, 1H), 8.17 (d, J = 8.2, 1H), 8.02 (s, 1H), 7.42–7.37 (m, 2H), 7.33–7.24 (m, 2H), 7.23–7.17 (m, 1H), 5.27–5.18 (m, 1H), 1.96–1.78 (m, 2H), 0.92 (t, J = 7.3, 3H); ^{13}C NMR (100 MHz, DMSO-d_6) δ: 166.5, 155.3, 154.1, 143.6, 128.3 (2C), 126.8, 126.5 (2C), 122.8, 116.8, 109.6, 55.5, 29.3, 11.4; IR (neat, cm^{-1}): 3048, 2963, 2872, 1599, 1474, 1363, 844, 756, 697; HRMS (ESI, m/z): 348.0165 (calcd. $C_{15}H_{15}^{79}BrN_3S$, 348.0165, $[M + H]^+$).

4.4.7. (rac)-6-Bromo-*N*-(2-methyl-1-phenylpropyl)thieno[2,3-d]pyrimidin-4-amine ((rac)-**18**)

The synthesis was performed as described in Section 4.4.1 starting with compound **1** (538 mg, 2.16 mmol) and 2-methyl-1-phenylpropan-1-amine ((*rac*)-**9**) (965 mg, 6.47 mmol). The reaction time was 18 h. The crude product was purified by silica-gel column chromatography (*n*-pentane/EtOAc, 1/1), R_f = 0.70. Drying gave 677 mg (1.81 mmol, 84%) of (*rac*)-**18** as an off white solid, mp 158–161 °C; HPLC purity: 97% (method A), t_R = 29.9 min; ^{1}H NMR (400 MHz, DMSO-d_6) δ: 8.27 (s, 1H), 8.11–8.09 (m, 1H), 8.05 (s, 1H), 7.43–7.41 (m, 2H), 7.33–7.29 (m, 2H), 7.22–7.19 (m, 1H), 5.06–5.02 (m, 1H), 2.22–2.10 (m, 1H), 1.03 (d, J = 6.6, 3H), 0.75 (d, J = 6.7, 3H); ^{13}C NMR (100 MHz, DMSO-d_6) δ: 166.9, 155.7, 154.5, 143.1, 128.6 (2C), 127.8 (2C), 127.2, 123.3, 117.2, 109.9, 60.7, 33.3, 20.4, 20.3; IR (neat, cm^{-1}): 3230, 2958, 1581, 1514, 699, 579; HRMS (APCI/ASAP, m/z): 362.0327 (calcd. $C_{16}H_{17}^{79}BrN_3S$, 362.0327, $[M + H]^+$).

4.4.8. (*R*)-6-Bromo-*N*-methyl-*N*-(1-phenylethyl)thieno[2,3-d]pyrimidin-4-amine ((*R*)-**19**)

The synthesis was performed as described in Section 4.4.1 starting with compound **1** (522 mg, 2.09 mmol) and (*R*)-*N*-methyl-1-phenylethanamine ((*R*)-**10**) (849 mg, 6.28 mmol). The reaction time was 18 h. The crude product was purified by silica-gel column chromatography (EtOAc/*n*-pentane, 4/1), R_f = 0.57. Isolation and drying gave 660 mg (1.90 mmol, 91%) of (*R*)-**19** as white solid, mp 249 °C (dec.); HPLC purity: 99% (method A), t_R = 30.7 min; $[\alpha]_D^{20}$ = −23.4 (*c* 1.04, DMSO); ^{1}H NMR (400 MHz, DMSO-d_6) δ: 8.37 (s, 1H), 7.78 (s, 1H), 7.38–7.27 (m, 5H), 6.40–6.35 (m, 1H), 3.03 (s, 3H), 1.59 (d, J = 7.0, 3H); ^{13}C NMR (100 MHz, DMSO-d_6) δ: 170.1, 157.0, 153.4, 141.1, 129.1 (2C), 127.6, 127.4 (2C), 125.9, 116.5, 108.8, 53.7, 33.5, 16.5; IR (neat, cm^{-1}): 2977, 1590, 1566, 1390, 760, 694; HRMS (APCI/ASAP, m/z): 348.0170 (calcd. $C_{15}H_{15}^{79}BrN_3S$, 348.0170, $[M + H]^+$).

4.4.9. (rac)-6-Bromo-*N*-(2,2,2-trifluoro-1-phenylethyl)thieno[2,3-d]pyrimidin-4-amine ((rac)-**20**)

The synthesis was performed as described in Section 4.4.1 starting with **1** (1.72 g, 6.91 mmol) and 2,2,2-trifluoro-1-phenylethanamine ((*rac*)-**11**) (3.63 g, 20.7 mmol) and reacting for 20 h. After drying over anhydrous Na_2SO_4 the concentrated black oil was dried under reduced pressure for 48 h. The obtained material was purified by silica-gel column chromatography (*n*-pentane/diethyl ether, 4/1), R_f = 0.21. Isolation and drying gave 1.60 g (4.12 mmol, 60%) of (*rac*)-**20** as a white solid, mp 204 °C (dec.); HPLC purity 99% (method A), t_R = 29.5 min; ^{1}H NMR (400 MHz, $CDCl_3$) δ: 8.49 (s, 1H), 7.48 (m, 2H), 7.43–7.38 (m, 3H), 7.28 (s, 1H), 6.38–6.32 (m, 1H), 5.72 (d, J = 9.2, 1H); ^{13}C NMR (100 MHz, $CDCl_3$) δ: 168.1, 154.2, 153.6, 133.0, 129.4, 129.1 (2C), 127.9 (2C), 124.7 (q, J = 211.3), 119.3, 117.3, 113.8, 54.9 (q, J = 31.3); ^{19}F NMR (564 MHz, DMSO-d_6) δ: −74.1 (s); IR (neat, cm^{-1}): 2996, 2359, 2341, 2159, 2029, 564; HRMS (EI, 70 eV, m/z): 387.9487, (calcd. $C_{14}H_9^{79}BrF_3N_3S$, 387.9487, $[M]^+$).

4.4.10. (rac)-6-Bromo-*N*-(2-fluoro-1-phenylethyl)thieno[2,3-d]pyrimidin-4-amine ((rac)-**21**)

Compound **1** (182 mg, 0.73 mmol) was mixed with 2-fluoro-1-phenylethan-1-amine ((*rac*)-**12**) (304 mg, 2.19 mmol) and 1-butanol (3 mL), and agitated at 50 °C for 72 h. Then the mixture was cooled to 25 °C, diluted with diethyl ether (20 mL) and washed with water (3 × 20 mL) and saturated aq NaCl solution (10 mL). After drying over Na_2SO_4 and concentration *in vacuo*, the obtained material was purified by silica-gel column chromatography (*n*-pentane/diethyl ether, 4/1), R_f = 0.24. This gave 205 mg (0.584 mmol, 80%) of (*rac*)-**21** as white solid, mp 135–137 °C (dec.); HPLC purity 96% (method A), t_R = 25.8 min; ^{1}H NMR (400 MHz, DMSO-d_6) δ: 8.49–8.47 (m, 1H), 8.31 (s, 1H), 8.04 (s, 1H), 7.49–7.47 (m, 2H), 7.38–7.34 (m, 2H), 7.30–7.27 (m, 1H), 5.81–5.72 (m, 1H), 4.81–4.75 (m, 1H), 4.69–4.64 (m, 1H); ^{13}C NMR (100 MHz, DMSO-d_6) δ: 167.2, 155.7, 154.4, 138.5 (d, J = 6.2), 128.9 (2C), 128.1, 127.6 (2C), 123.2, 117.4, 110.5, 84.7 (d, J = 174.7), 54.2 (d, J = 19.9); ^{19}F NMR (564 MHz, DMSO-d_6) δ: −220.1 (s); IR (neat, cm^{-1}): 3216, 3073, 3009, 1585, 1540, 1445, 1017, 693; HRMS (EI, 70 eV, m/z): 350.9831, (calcd. $C_{14}H_{11}^{79}BrFN_3S$, 350.9831, $[M]^+$).

4.4.11. (*S*)-6-Bromo-*N*-(2-methoxy-1-phenylethyl)thieno[2,3-d]pyrimidin-4-amine ((*S*)-**22**)

The synthesis was performed as described in Section 4.4.1 starting with compound **1** (213 mg, 0.854 mmol) and (*S*)-2-methoxy-1-phenylethanamine ((*S*)-**13**) (387 mg, 2.56 mmol). The reaction time was 22 h. The crude product was purified by silica-gel column chromatography (*n*-pentane/EtOAc, 1/1), R_f = 0.63. Isolation and drying gave 238 mg (0.653 mmol, 77%) of (*S*)-**22** as an off-white solid, mp 158–160 °C; HPLC purity: 99% (method A), t_R = 25.0 min; $[\alpha]_D^{20}$ = −246.9 (*c* 0.79, DMSO); ^{1}H NMR (400 MHz, DMSO-d_6) δ: 8.31 (br s, 1H), 8.28 (s, 1H), 8.05 (s, 1H), 7.44–7.42 (m, 2H), 7.35–7.31 (m, 2H), 7.26–7.23 (m, 1H), 5.64–5.59 (m, 1H), 3.72 (dd_{AB}, J = 10.1, 8.8, 1H), 3.62 (dd_{AB}, J = 10.1, 5.1, 1H), 3.30 (s, 3H); ^{13}C NMR (100 MHz, DMSO-d_6) δ: 167.0, 155.7, 154.5, 140.7, 128.8 (2C), 127.6, 127.4 (2C), 123.3, 117.3, 110.2, 75.1, 58.5, 53.7; IR (neat, cm^{-1}): 3363, 2888, 1575, 1536, 1494, 1096, 702; HRMS (APCI/ASAP, m/z): 364.0119 (calcd. $C_{15}H_{15}^{79}BrN_3OS$, 364.0119, $[M + H]^+$).

4.4.12. (*R*)-6-Bromo-*N*-(2-methoxy-1-phenylethyl)thieno[2,3-d]pyrimidin-4-amine ((*R*)-**22**)

The synthesis was performed as described in Section 4.4.11 starting with compound **1** (535 mg, 2.15 mmol) and (*R*)-2-methoxy-1-phenylethanamine ((*R*)-**13**) (973 mg, 6.44 mmol). The reaction time was 21 h. This gave 696 mg (1.85 mmol, 85%) of (*R*)-**22** as an off-white solid, mp 157–160 °C; HPLC purity: 98% (method A),

t_R = 24.9 min; $[\alpha]_D^{20}$ = 199.4 (*c* 0.68, DMSO); ^{1}H NMR (400 MHz, DMSO-d_6) δ: 8.30 (br s, 1H), 8.28 (s, 1H), 8.04 (s, 1H), 7.44–7.42 (m, 2H), 7.35–7.31 (m, 2H), 7.26–7.23 (m, 1H), 5.64–5.58 (m, 1H), 3.75–3.62 (m, 2H), 3.30 (s, 3H); HRMS (APCI/ASAP, *m*/*z*): 364.0120 (calcd. $C_{15}H_{15}^{79}BrN_3OS$, 364.0119, $[M + H]^+$). The spectroscopic properties confirmed with that reported for (*S*)-**22**.

4.4.13. (*R*)-2-((6-Bromothieno[2,3-d]pyrimidin-4-yl)amino)-2-phenylethanol ((*R*)-**23**)

The synthesis was performed as described in Section 4.4.1 starting with compound **1** (300 mg, 1.20 mmol) and (*R*)-2-amino-2-phenylethan-1-ol ((*R*)-**14**) (495 mg, 3.61 mmol). The reaction time was 24 h. The crude product was purified by silica-gel column chromatography (EtOAc), R_f = 0.71. Isolation and drying gave 346 mg (0.988 mmol, 82%) of (*R*)-**23** as a white solid, mp 171–173 °C; HPLC purity: 96% (method A), t_R = 20.6 min; $[\alpha]_D^{20}$ = 196.4 (*c* 0.59, DMSO); ^{1}H NMR (400 MHz, DMSO-d_6) δ: 8.26 (s, 1H), 8.20–8.18 (m, 1H), 8.04 (s, 1H), 7.42–7.40 (m, 2H), 7.33–7.29 (m, 2H), 7.24–7.21 (m, 1H), 5.44–5.38 (m, 1H), 5.03–5.00 (m, 1H), 3.78–3.68 (m, 2H); ^{13}C NMR (100 MHz, DMSO-d_6) δ: 166.9, 155.9, 154.5, 141.3, 128.7 (2C), 127.4 (3C), 123.4, 117.4, 109.9, 65.1, 56.9; IR (neat, cm^{-1}): 3421, 3042, 1602, 1477, 1357, 698; HRMS (APCI/ASAP, *m*/*z*): 349.9966 (calcd. $C_{14}H_{13}^{79}BrN_3OS$, 349.9963, $[M + H]^+$).

4.4.14. (*S*)-2-((6-Bromothieno[2,3-d]pyrimidin-4-yl)amino)-2-phenylethanol ((*S*)-**23**)

The synthesis was performed as described in Section 4.4.13 starting with compound **1** (300 mg, 1.20 mmol) and (*S*)-2-amino-2-phenylethan-1-ol ((*S*)-**14**) (495 mg, 3.61 mmol). The reaction time was 24 h. The crude product was purified by silica-gel column chromatography (*n*-pentane/EtOAc, 2/8), R_f = 0.58. This gave 360 mg (1.03 mmol, 86%) of (*S*)-**23** as a white solid, mp 169–172 °C; HPLC purity: 98% (method A), t_R = 20.6 min; $[\alpha]_D^{20}$ = −210.4 (*c* 0.73, DMSO); ^{1}H NMR (400 MHz, DMSO-d_6) δ: 8.26 (s, 1H), 8.20–8.18 (m, 1H), 8.04 (s, 1H), 7.42–7.40 (m, 2H), 7.33–7.29 (m, 2H), 7.24–7.21 (m, 1H), 5.44–5.38 (m, 1H), 5.03–5.00 (m, 1H), 3.78–3.68 (m, 2H); HRMS (APCI/ASAP, *m*/*z*): 349.9966 (calcd. $C_{14}H_{13}^{79}BrN_3OS$, 349.9963, $[M + H]^+$). The spectroscopic properties confirmed with that reported for (*R*)-**23**.

4.5. 4-Chloro-6-(4-fluorophenyl)thieno[2,3-d]pyrimidine (***24c***) [69]

Compound **1** (1.00 g, 4.02 mmol) was mixed with (4-fluorophenyl)boronic acid (**4c**) (844 mg, 6.03 mmol), fine powdered K_2CO_3 (1.68 g, 12.1 mmol), $Pd_2(dba)_3$ (186 mg, 0.20 mmol) and 1,4-dioxane (20 mL). The reaction was then stirred at 110 °C for 26 h under N_2 atmosphere. The solvent was removed and the product was dissolved in diethyl ether (150 mL) and washed with water (3 × 150 mL). The organic phase was dried over anhydrous Na_2SO_4, filtered and concentrated *in vacuo*. The crude product was absorbed onto silica and purified by silica-gel column chromatography (*n*-pentane/acetone, 19/1), R_f = 0.28. Drying gave 415 mg (1.57 mmol, 39%) of **24c** as a pale white solid, mp 142–143 °C; HPLC purity: 91% (method B), t_R = 23.5 min; ^{1}H NMR (400 MHz, DMSO-d_6) δ: 8.93 (s, 1H), 8.04–7.98 (m, 3H), 7.43–7.36 (m, 2H); ^{13}C NMR (100 MHz, DMSO-d_6) δ: 167.6, 163.0 (d, J = 248.6), 153.3, 152.8, 144.1, 130.8, 129.2 (d, J = 8.7, 2C), 128.5 (d, J = 3.1), 116.5 (d, J = 22.0, 2C), 115.1; ^{19}F NMR (564 MHz, DMSO-d_6) δ: −115.3 (s); IR (neat, cm^{-1}): 3063, 1884, 1505, 1429, 1228, 1165, 813, 759, 670; HRMS (ESI, *m*/*z*): 264.9995 (calcd. $C_{12}H_7^{35}ClN_2S$, 264.9997, $[M + H]^+$).

4.6. Synthesis of potential EGFR inhibitors

The synthesis and spectral properties of the compounds (*R*)-**5a**, (*R*)-**5b**, (*R*)-**5d**, (*R*)-**5h**, (*R*)-**5j**, (*R*)-**5n**, (*R*)-**5u** and (*R*)-**5v** have been described earlier [25].

4.6.1. General procedure for Suzuki coupling on 6-bromothieno[2,3-d]pyrimidines

Compound (*R*)-**3**·HCl (201 mg, 0.54 mmol) was mixed with the selected boronic acid (**4**) (0.81 mmol), fine powdered K_2CO_3 (298 mg, 2.16 mmol), $Pd(PPh_3)_4$ (6 mg, 0.005 mmol), 1,4-dioxane (2 mL) and water (2 mL). The reaction was then stirred at 80 °C for 2–3 h under N_2 atmosphere. The solvent was removed and the product was diluted with water (20 mL) and extracted with diethyl ether or EtOAc (25 mL), the water phase was extracted with more diethyl ether or EtOAc (3 × 10 mL). The combined organic phases were washed with saturated aq NaCl solution (10 mL), dried over anhydrous Na_2SO_4, filtered and concentrated *in vacuo*. Purification was performed as specified for each individual compound.

4.6.2. (*S*)-6-Phenyl-N-(1-phenylethyl)thieno[2,3-d]pyrimidin-4-amine ((*S*)-***5a***)

4-Chloro-6-phenylthieno[2,3-*d*]pyrimidine (**24a**) [25] (30 mg, 0.122 mmol) and (*S*)-phenylethanamine ((*S*)-**2**) (45 mg, 0.371 mmol) were added to 1-butanol (1 mL) under N_2 atmosphere and heated at 145 °C for 24 h. After cooling to rt, 1-butanol was evaporated *in vacuo*, and water (10 mL) was added. The mixture was extracted with EtOAc (3 × 10 mL). The combined organic phases were washed with saturated aq NaCl solution (10 mL) and dried over anhydrous Na_2SO_4, filtrated and evaporated. The obtained material was purified by silica-gel column chromatography (*n*-pentane/EtOAc, 1/1), R_f = 0.76. This gave 32 mg (0.097 mmol, 79%) of (*S*)-**5a** as a white solid, mp 171–173 °C; HPLC purity: 99% (method A), t_R = 32.1 min, ee: 99% t_R = 7.8 min (Lux 5u Cellulose-1); $[\alpha]_D^{20}$ = 272.1 (*c* 0.72, DMSO); ^{1}H NMR (400 MHz, DMSO-d_6) δ: 8.28 (s, 1H), 8.24 (d, J = 7.9, 1H), 8.21 (s, 1H), 7.71–7.69 (m, 2H), 7.54–7.48 (m, 2H), 7.46–7.37 (m, 3H), 7.35–7.30 (m, 2H), 7.25–7.20 (m, 1H), 5.56–5.47 (m, 1H), 1.56 (d, J = 7.1, 3H). HRMS (APCI/ASAP, *m*/*z*): 331.1142 (calcd. $C_{20}H_{18}N_3S$, 331.1143, $[M + H]^+$). Other spectroscopic properties were identical to that of the (*R*)-**5a** reported previously [25].

4.6.3. (*R*)-6-(4-Fluorophenyl)-N-(1-phenylethyl)thieno[2,3-d]pyrimidin-4-amine hydrochloride ((*R*)-***5c***·HCl)

Compound **24c** (99 mg, 0.374 mmol) was mixed with (*R*)-1-phenylethanamine ((*R*)-**2**) (0.15 mL, 143 mg, 1.18 mmol) and 1-butanol (2 mL), and agitated at 145 °C for 21 h. Then the mixture was cooled to rt, diluted with EtOAc (40 mL) and washed with water (3 × 15 mL). The combined organic phases was dried over anhydrous Na_2SO_4, filtered and concentrated *in vacuo*. The crude product was absorbed onto silica and purified with silica-gel column chromatography (*n*-pentane/EtOAc, 3/1), R_f = 0.20. The product was precipitated from diethyl ether (50 mL)/HCl in diethyl ether (1.5 mL) at −18 °C for 24 h. The solid formed was isolated by filtration and washed with diethyl ether (2 × 25 mL). Drying gave 57 mg (0.148 mmol, 40%) of (*R*)-**5c**·HCl as a white solid, mp 182–187 °C; HPLC purity: 99% (method B), t_R = 18.6 min; $[\alpha]_D^{20}$ = −280.7 (*c* 0.97, DMSO); ^{1}H NMR (400 MHz, DMSO-d_6) δ: 8.28 (s, 1H), 8.25 (d, J = 7.9, 1H), 8.15 (s, 1H), 7.80–7.68 (m, 2H), 7.47–7.40 (m, 2H), 7.40–7.28 (m, 4H), 7.27–7.19 (m, 1H), 5.56–5.47 (m, 1H), 1.56 (d, J = 7.0, 3H); ^{13}C NMR (100 MHz, DMSO-d_6) δ: 165.2, 162.1 (d, J = 246.1), 155.8, 153.9, 144.6, 136.9, 129.9 (d, J = 3.0), 128.3 (2C), 127.8 (d, J = 8.5, 2C), 126.7, 126.1 (2C), 117.4, 116.4 (d, J = 22.0, 2C), 115.7, 49.1, 22.5; ^{19}F NMR (564 MHz, DMSO-d_6) δ: −115.4 (s); IR (neat, cm^{-1}): 3059, 2978, 1604, 1491, 1233, 832, 766, 699; HRMS (ESI, *m*/*z*): 350.1122 (calcd. $C_{20}H_{17}FN_3S$, 350.1122, $[M + H]^+$).

4.6.4. (*R*)-(4-(4-((1-Phenylethyl)amino)thieno[2,3-d]pyrimidin-6-yl)phenyl)methanol ((*R*)-***5e***)

Compound (*R*)-**3**·HCl (201 mg, 0.542 mmol) was mixed with the MIDA boronate ester of 4-(hydroxymethyl)phenylboronic acid (**4e**)

(215 mg, 0.817 mmol), SPhos (22 mg, 0.054 mmol), $Pd(OAc)_2$ (8.5 mg, 0.038 mmol) and 1,4-dioxane (5 mL). The mixture was stirred for 10 min, 3 M K_3PO_4 solution (1.5 mL) was added and the temperature increased to 80 °C for 3 h under an N_2 atmosphere. The reaction mixture was cooled to rt and added 1 M NaOH solution (5 mL) and diethyl ether (25 mL). The water phase was extracted with diethyl ether (2 × 10 mL). The combined organic phases were dried over anhydrous Na_2SO_4, filtered and concentrated *in vacuo*. The crude product was absorbed onto silica and purified with silica-gel column chromatography (*n*-pentane/EtOAc, 11/9), R_f = 0.17. Drying gave 95 mg (0.262 mmol, 48%) of (*R*)-**5e** as a white solid, mp 215–217 °C; HPLC purity: 99% (method B), t_R = 21.9 min; $[\alpha]_D^{20}$ = −255.2 (*c* 0.97, DMSO); ^{1}H NMR (400 MHz, DMSO-d_6) δ: 8.28 (s, 1H), 8.22 (d, J = 7.9, 1H), 8.18 (s, 1H), 7.68–7.64 (m, 2H), 7.47–7.41 (m, 4H), 7.36–7.30 (m, 2H), 7.25–7.19 (m, 1H), 5.56–5.47 (m, 1H), 5.29 (t, J = 5.8, 1H), 4.55 (d, J = 5.7, 2H), 1.57 (d, J = 7.1, 3H); ^{13}C NMR (100 MHz, DMSO-d_6) δ: 165.0, 155.7, 153.8, 144.6, 143.2, 138.2, 131.6, 128.3 (2C), 127.3 (2C), 126.7, 126.1 (2C), 125.4 (2C), 117.5, 115.1, 62.5, 49.0, 22.5; IR (neat, cm^{-1}): 3246, 3142, 2860, 1578, 1493, 1313, 1102, 777, 694; HRMS (EI, 70 eV, *m*/*z*): 361.1242 (calcd. $C_{21}H_{19}N_3OS$, 361.1243, $[M]^+$).

4.6.5. (*R*)-*N*-(1-Phenylethyl)-6-(*p*-tolyl)thieno[2,3-*d*]pyrimidin-4-amine ((*R*)-**5f**)

Compound (*R*)-**5f** was prepared as described in Section 4.6.1, but starting with *p*-tolylboronic acid (**4f**) (110 mg, 0.816 mmol). The reaction time was 2 h. The crude product was purified by silica-gel column chromatography (*n*-pentane/EtOAc, 3/1), R_f = 0.29. Drying gave 162 mg (0.467 mmol, 86%) of (*R*)-**5f** as a pale yellow solid, mp 78–81 °C; HPLC purity: 99% (method B), t_R = 27.7 min; $[\alpha]_D^{20}$ = −413.1 (*c* 1.02, DMSO); ^{1}H NMR (400 MHz, DMSO-d_6) δ: 8.27 (s, 1H), 8.20 (d, J = 7.9, 1H), 8.14 (s, 1H), 7.61–7.57 (m, 2H), 7.45–7.41 (m, 2H), 7.35–7.29 (m, 4H), 7.25–7.19 (m, 1H), 5.56–5.47 (m, 1H), 2.35 (s, 3H), 1.57 (s, J = 7.0, 3H); ^{13}C NMR (100 MHz, DMSO-d_6) δ: 164.9, 155.7, 153.7, 144.6, 138.3, 138.2, 130.5, 129.9 (2C), 128.3 (2C), 126.7, 126.1 (2C), 125.5 (2C), 117.5, 114.8, 49.0, 22.5, 20.8; IR (neat, cm^{-1}): 3259, 2973, 1576, 1493, 1351, 810, 775, 697; HRMS (EI, 70 eV, *m*/*z*): 345.1292 (calcd. $C_{21}H_{19}N_3S$, 345.1294, $[M]^+$).

4.6.6. (*R*)-6-(4-(tert-Butyl)phenyl)-*N*-(1-phenylethyl)thieno[2,3-*d*]pyrimidin-4-amine ((*R*)-**5g**)

Compound (*R*)-**5g** was prepared as described in Section 4.6.1, but starting with (4-(*tert*-butyl)phenyl)boronic acid (**4g**) (123 mg, 0.691 mmol). The reaction time was 3 h at 60 °C. The crude product was absorbed onto silica and purified by silica-gel column chromatography (*n*-pentane/EtOAc, 3/1), R_f = 0.24. The purified product was dissolved in diethyl ether (100 mL), *n*-pentane was added to the mixture until the product precipitated. Filtration and drying gave 145 mg (0.374 mmol, 69%) of (*R*)-**5g** as a white solid, mp 165–166 °C; HPLC purity: 98% (method A), t_R = 35.9 min; $[\alpha]_D^{20}$ = −305.1 (c 0.37, DMSO); ^{1}H NMR (300 MHz, DMSO-d_6) δ: 8.27 (s, 1H), 8.24 (d, J = 7.9, 1H), 8.14 (s, 1H), 7.64–7.62 (m, 2H), 7.53–7.51 (m, 2H), 7.44–7.42 (m, 2H), 7.35–7.31 (m, 2H), 7.24–7.20 (m, 1H), 5.55–5.48 (m, 1H), 1.57 (d, J = 7.0, 3H), 1.32 (s, 9H); ^{13}C NMR (100 MHz, DMSO-d_6) δ: 164.9, 155.7, 153.8, 151.3, 144.6, 138.2, 130.5, 128.3 (2C), 126.7, 126.2 (2C), 126.1 (2C), 125.4 (2C), 117.5, 114.8, 49.0, 34.5, 31.0 (3C), 22.5; IR (neat, cm^{-1}): 3265, 2960, 1575, 1521, 1493, 1351, 1306, 1104, 827, 776, 697, 554; HRMS (APCI/ASAP, *m*/*z*): 388.1843 (calcd. $C_{24}H_{26}N_3S$, 388.1847, $[M + H]^+$).

4.6.7. (*R*)-4-(4-((1-phenylethyl)amino)thieno[2,3-*d*]pyrimidin-6-yl)benzaldehyde ((*R*)-**5i**)

Compound (*R*)-**5i** was prepared as described in Section 4.6.1, but starting with (4-formylphenyl)boronic acid (**4i**) (163 mg, 1.09 mmol). The reaction time was 19 h at 60 °C. The crude product was absorbed onto silica and purified by silica-gel column chromatography (*n*-pentane/EtOAc, 3/2), R_f = 0.28. The purified product was recrystallized from acetonitrile. Filtration and drying gave 15 mg (0.042 mmol, 30%) of (*R*)-**5i** as a yellow solid, mp 210–218 °C; HPLC purity: 99% (method A), t_R = 28.0 min; $[\alpha]_D^{20}$ = −506.2 (c 0.52, DMSO); ^{1}H NMR (400 MHz, DMSO-d_6) δ: 10.04 (s, 1H), 8.42 (s, 1H), 8.32 (s, 1H), 8.36 (d, J = 7.9, 1H), 8.05–8.03 (m, 2H), 7.92–7.90 (m, 2H), 7.45–7.43 (m, 2H), 7.35–7.31 (m, 2H), 7.25–7.21 (m, 1H), 5.56–5.49 (m, 1H), 1.58 (d, J = 7.0, 3H); ^{13}C NMR (100 MHz, DMSO-d_6) δ: 192.3, 165.9, 156.0, 154.5, 144.4, 138.7, 136.4, 135.5, 130.6 (2C), 128.3 (2C), 126.8, 126.1 (2C), 126.0 (2C), 118.2, 117.4, 49.1, 22.5; IR (neat, cm^{-1}): 3369, 2973, 1683, 1575, 1491, 1116, 816, 775, 698, 553; HRMS (APCI/ASAP, *m*/*z*): 360.1169 (calcd. $C_{21}H_{18}N_3OS$, 360.1171, $[M + H]^+$).

4.6.8. (*R*)-6-(3-Methoxyphenyl)-*N*-(1-phenylethyl)thieno[2,3-*d*]pyrimidin-4-amine ((*R*)-**5k**)

Compound (*R*)-**5k** was prepared as described in Section 4.6.4, but starting with the MIDA boronate ester of (3-methoxyphenyl) boronic acid (**4k**) (287 mg, 1.09 mmol). The reaction time was 3 h. The crude product was absorbed onto silica and purified by silica-gel column chromatography (*n*-pentane/EtOAc, 7/3), R_f = 0.26. Drying gave 114 mg (0.315 mmol, 58%) of (*R*)-**5k** as a pale yellow solid, mp 135–137 °C; HPLC purity: 99% (method B), t_R = 26.9 min; $[\alpha]_D^{20}$ = −336.4 (*c* 1.01, DMSO); ^{1}H NMR (400 MHz, DMSO-d_6) δ: 8.29 (s, 1H), 8.22 (d, J = 7.9, 1H), 8.19 (s, 1H), 7.46–7.39 (m, 3H), 7.36–7.30 (m, 2H), 7.29–7.20 (m, 3H), 7.01–6.97 (m, 1H), 5.57–5.48 (m, 1H), 3.85 (s, 3H), 1.57 (d, J = 7.1, 3H); ^{13}C NMR (100 MHz, DMSO-d_6) δ: 165.1, 159.9, 155.8, 154.0, 144.6, 137.9, 134.6, 130.5, 128.3 (2C), 126.7, 126.1 (2C), 118.2, 117.3, 115.8, 114.2, 110.9, 55.3, 49.0, 22.5; IR (neat, cm^{-1}): 3230, 1577, 1514, 1491, 1289, 780, 699; HRMS (EI, 70 eV, *m*/*z*): 361.1241 (calcd. $C_{21}H_{19}N_3OS$, 361.1243, $[M]^+$).

4.6.9. (*R*)-(3-(4-((1-Phenylethyl)amino)thieno[2,3-*d*]pyrimidin-6-yl)phenyl)methanol ((*R*)-**5l**)

Compound (*R*)-**5l** was prepared as described in Section 4.6.1, but starting with (3-(hydroxymethyl)phenyl)boronic acid (**4l**) (99 mg, 0.646 mmol). The reaction time was 3 h. The crude product was absorbed onto silica and purified with silica-gel column chromatography (*n*-pentane/EtOAc, 7/3), R_f = 0.67 (EtOAc). The resulting product was dissolved in diethyl ether (2 mL), and slowly added to *n*-pentane (30 mL) to give precipitation. Isolation and drying gave 140 mg (0.387 mmol, 90%) of (*R*)-**5l** as a white solid, mp 173–176 °C; HPLC purity: 98% (method A), t_R = 27.0 min; $[\alpha]_D^{20}$ = −302.7 (*c* 0.83, DMSO); ^{1}H NMR (400 MHz, DMSO-d_6) δ: 8.29–8.27 (m, 2H), 8.23 (s, 1H), 7.72 (s, 1H), 7.56–7.54 (m, 1H), 7.47–7.43 (m, 3H), 7.35–7.31 (m, 3H), 7.24–7.21 (m, 1H), 5.55–5.48 (m, 1H), 5.37–5.34 (m, 1H), 4.60–4.58 (m, 2H), 1.57 (d, J = 7.0, 3H); ^{13}C NMR (100 MHz, DMSO-d_6) δ: 165.5, 155.7, 153.9, 145.1, 144.3, 138.8, 133.5, 129.6, 128.8 (2C), 127.2, 127.0, 126.5 (2C), 124.5, 123.7, 117.9, 115.9, 63.0, 49.5, 23.0; IR (neat, cm^{-1}): 3309, 1584, 998, 759, 702; HRMS (APCI/ASAP, *m*/*z*): 362.1324 (calcd. $C_{21}H_{20}N_3OS$, 362.1325, $[M + H]^+$).

4.6.10. (*R*)-*N*-(1-Phenylethyl)-6-(*m*-tolyl)thieno[2,3-*d*]pyrimidin-4-amine ((*R*)-**5m**)

Compound (*R*)-**5m** was prepared as described in Section 4.6.4, but starting with the MIDA boronate ester of *m*-tolylboronic acid (**4m**) (205 mg, 0.831 mmol). The reaction time was 3 h. The crude product was purified by silica-gel column chromatography (*n*-pentane/EtOAc, 3/1), R_f = 0.46. Drying gave 127 mg (0.368 mmol, 68%) of (*R*)-**5m** as a pale yellow solid, mp 82–85 °C; HPLC purity: 99% (method B), t_R = 27.8 min; $[\alpha]_D^{20}$ = −443.5 (*c* 1.03, DMSO); ^{1}H NMR (400 MHz, DMSO-d_6) δ: 8.25 (s, 1H), 8.23 (d, J = 7.9, 1H), 8.19 (s, 1H), 7.54–7.52 (m, 1H), 7.50–7.46 (m, 1H), 7.45–7.41 (m, 2H), 7.41–7.36 (m, 1H), 7.35–7.30 (m, 2H), 7.25–7.19 (m, 2H), 5.56–5.47

(m, 1H), 2.39 (s, 3H), 1.57 (d, $J = 7.1$, 3H); ^{13}C NMR (100 MHz, DMSO-d_6) δ: 165.0, 155.7, 153.9, 144.6, 138.6, 138.2, 133.1, 129.27, 129.25, 128.3 (2C), 126.7, 126.1 (3C), 122.9, 117.4, 115.4, 49.0, 22.5, 21.0; IR (neat, cm^{-1}): 3259, 2973, 1577, 1513, 1350, 772, 697; HRMS (EI, 70 eV, *m/z*): 345.1291 (calcd. $C_{21}H_{19}N_3S$, 345.1294, $[M]^+$).

4.6.11. (S)-2-(4-((1-Phenylethyl)amino)thieno[2,3-d]pyrimidin-6-yl)phenol ((S)-**5n**)

Compound (*S*)-**5n** was prepared as described in Section 4.6.1, but starting with (*S*)-**3** (150 mg, 0.449 mmol) and (2-hydroxyphenyl)boronic acid (**4n**) (93 mg, 0.673 mmol), and reacting for 4 h. The crude product was purified by silica-gel column chromatography (CH_2Cl_2/MeOH, 19/1), $R_f = 0.45$. The purified product was dissolved in diethyl ether (2 mL), slowly added to *n*-pentane (30 mL) to give precipitation. This gave 136 mg (0.393 mmol, 87%) of (*S*)-**5n** as a pale white solid, mp 227–230 °C; HPLC purity: 96% (method A), $t_R = 28.0$ min; $[\alpha]_D^{20} = 287.2$ (*c* 0.80, DMSO); ^{1}H NMR (400 MHz, DMSO-d_6) δ: 10.41 (s, 1H), 8.62 (s, 1H), 8.23 (s, 1H), 8.22 (d, $J = 8.0$, 1H), 7.69–7.65 (m, 1H), 7.44–7.41 (m, 2H), 7.34–7.29 (m, 2H), 7.24–7.18 (m, 2H), 7.03–6.99 (m, 1H), 6.97–6.91 (m, 1H), 5.57–5.51 (m, 1H), 1.56 (d, $J = 7.1$, 3H); HRMS (APCI/ASAP, *m/z*): 348.1167 (calcd. $C_{20}H_{18}N_3OS$, 348.1171, $[M + H]^+$). Other spectroscopic properties were identical to that of the (*R*)-**5n** reported previously [25].

4.6.12. (R)-6-(2-Aminophenyl)-N-(1-phenylethyl)thieno[2,3-d]pyrimidin-4-amine ((R)-**5o**)

Compound (*R*)-**5o** was prepared as described in Section 4.6.1, but starting with (2-aminophenyl)boronic acid hydrochloride (**4o**·HCl) (140 mg, 0.805 mmol). The reaction time was 17 h. The crude product was purified by silica-gel column chromatography (*n*-pentane/EtOAc, 1/1), $R_f = 0.37$. Drying gave 158 mg (0.455 mmol, 84%) of (*R*)-**5o** as a dark orange solid, mp 68–72 °C; HPLC purity: 97% (method B), $t_R = 15.1$ min; $[\alpha]_D^{20} = -336.2$ (*c* 0.53, DMSO); ^{1}H NMR (400 MHz, DMSO-d_6) δ: 8.27 (s, 1H), 8.20 (d, $J = 7.9$, 1H), 7.91 (s, 1H), 7.45–7.41 (m, 2H), 7.35–7.29 (m, 2H), 7.25–7.19 (m, 2H), 7.13–7.08 (m, 1H), 6.86–6.82 (m, 1H), 6.68–6.63 (m, 1H), 5.57–5.47 (m, 1H), 5.32 (s, 2H), 1.56 (d, $J = 7.0$, 3H); ^{13}C NMR (100 MHz, DMSO-d_6) δ: 164.9, 155.6, 153.4, 145.8, 144.8, 136.7, 130.2, 129.4, 128.3 (2C), 126.6, 126.1 (2C), 117.5, 117.2, 117.1, 116.7, 116.0, 49.0, 22.5; IR (neat, cm^{-1}): 3311, 3025, 2972, 1575, 1490, 1349, 1302, 747, 698; HRMS (EI, 70 eV, *m/z*): 346.1243 (calcd. $C_{20}H_{18}N_4S$, 346.1247, $[M]^+$).

4.6.13. (R)-6-(2-Methoxyphenyl)-N-(1-phenylethyl)thieno[2,3-d]pyrimidin-4-amine ((R)-**5p**)

Compound (*R*)-**5p** was prepared as described in Section 4.6.1, but starting with (2-methoxyphenyl)boronic acid (**4p**) (93 mg, 0.605 mmol). The reaction time was 3 h. The crude product was absorbed onto silica and purified by silica-gel column chromatography (*n*-pentane/EtOAc, 4/1), $R_f = 0.53$. The resulting product was dissolved in diethyl ether (2 mL) and slowly added to *n*-pentane (30 mL) to give precipitation. Isolation and drying gave 122 mg (0.387 mmol, 84%) of (*R*)-**5p** as a white solid, mp 158–161 °C; HPLC purity: 98% (method A), $t_R = 23.7$ min; $[\alpha]_D^{20} = -300.3$ (*c* 1.03, DMSO); ^{1}H NMR (400 MHz, DMSO-d_6) δ: 8.32 (s, 1H), 8.29 (s, 1H), 8.25 (d, $J = 8.0$, 1H), 7.81–7.78 (m, 1H), 7.49–7.46 (m, 2H), 7.45–7.40 (m, 1H), 7.38–7.34 (m, 2H), 7.28–7.22 (m, 2H), 7.17–7.12 (m, 1H), 5.58–5.48 (m, 1H), 3.99 (s, 3H), 1.62 (d, $J = 7.2$, 3H); ^{13}C NMR (100 MHz, DMSO-d_6) δ: 166.1, 156.1, 155.9, 154.2, 145.2, 134.4, 130.2, 128.8 (2C), 128.4, 127.1, 126.6 (2C), 122.3, 121.5, 117.5, 116.6, 113.0, 56.3, 49.4, 22.9; IR (neat, cm^{-1}): 2359, 1609, 751, 699; HRMS (EI, 70 eV, *m/z*): 361.1241 (calcd. $C_{21}H_{19}ON_3S$, 361.1243, $[M]^+$).

4.6.14. (R)-(2-(4-((1-Phenylethyl)amino)thieno[2,3-d]pyrimidin-6-yl)phenyl)methanol ((R)-**5q**)

Compound (*R*)-**5q** was prepared as described in Section 4.6.1, but starting with compound (2-(hydroxymethyl)phenyl)boronic acid (**4q**) (94 mg, 0.618 mmol), and reacting for 5 h. The crude product was purified by silica-gel column chromatography (EtOAc/*n*-pentane, 7/3), $R_f = 0.60$. The purified product was then dissolved in diethyl ether (2 mL) and slowly added to *n*-pentane (30 mL) to give precipitation. Isolation and drying gave 141 mg (0.390 mmol, 95%) of (*R*)-**5q** as a white solid, mp 137–139 °C; HPLC purity: 97% (method A), $t_R = 27.2$ min; $[\alpha]_D^{20} = -294.2$ (*c* 0.67, DMSO); ^{1}H NMR (400 MHz, DMSO-d_6) δ: 8.31 (s, 1H), 8.27–8.25 (m, 1H), 7.81 (s, 1H), 7.49–7.31 (m, 9H), 5.58–5.50 (m, 1H), 5.34 (s, br, 1H), 4.71 (s, 2H), 1.57 (d, $J = 7.0$, 3H); ^{13}C NMR (100 MHz, DMSO-d_6) δ: 165.6, 155.8, 153.7, 144.6, 140.2, 136.4, 131.5, 130.5, 130.0, 128.5, 128.3 (2C), 127.8, 127.1, 126.7, 126.0 (2C), 116.8, 60.9, 49.0, 22.4; IR (neat, cm^{-1}): 3313, 2974, 1581, 1494, 1352, 996, 761; HRMS (APCI/ASAP, *m/z*): 362.1326 (calcd. $C_{21}H_{20}N_3OS$, 362.1325, $[M + H]^+$).

4.6.15. (R)-N-(1-Phenylethyl)-6-(o-tolyl)thieno[2,3-d]pyrimidin-4-amine ((R)-**5r**)

The MIDA boronate ester of *o*-tolylboronic acid (**4r**) (240 mg, 0.971 mmol) was dissolved in THF (10 mL). 1 M NaOH solution (3 mL) was added and the mixture was stirred for 25 min. The mixture was diluted with 0.5 M pH 7 sodium phosphate buffer (10 mL) and diethyl ether (10 mL). The aqueous phase was extracted with THF/diethyl ether 1/1 (2 × 10 mL). The combined organic phases were dried over anhydrous Na_2SO_4, filtered and concentrated *in vacuo*. Drying gave 108 mg (0.797 mmol, 82%) of **4r** as a white solid. The freshly prepared *o*-tolylboronic acid (**4r**) (108 mg, 0.797 mmol) was used in a cross-coupling reaction as described in Section 4.6.1. The reaction time was 17 h. The crude product was absorbed onto silica and purified by silica-gel column chromatography (*n*-pentane/EtOAc, 3/1), $R_f = 0.29$. Drying gave 151 mg (0.438 mmol, 81%) of (*R*)-**5r** as a pale yellow solid, mp 79–83 °C; HPLC purity: 99% (method B), $t_R = 26.8$ min; $[\alpha]_D^{20} = -309.8$ (*c* 1.06, DMSO); ^{1}H NMR (400 MHz, DMSO-d_6) δ: 8.30 (s, 1H), 8.24 (d, $J = 7.9$, 1H), 7.86 (s, 1H), 7.50–7.46 (m, 1H), 7.45–7.41 (m, 2H), 7.40–7.29 (m, 5H), 7.25–7.19 (m, 1H), 5.57–5.50 (m, 1H), 2.49 (s, 3H), 1.57 (d, $J = 7.0$, 3H); ^{13}C NMR (100 MHz, DMSO-d_6) δ: 165.5, 155.9, 153.7, 144.6, 137.5, 135.5, 133.0, 131.2, 130.1, 128.6, 128.3 (2C), 126.7, 126.4, 126.1 (2C), 118.8, 116.8, 49.0, 22.4, 21.0; IR (neat, cm^{-1}): 3255, 2972, 1576, 1513, 1348, 755, 697; HRMS (EI, 70 eV, *m/z*): 345.1294 (calcd. $C_{21}H_{19}N_3S$, 345.1294, $[M]^+$).

4.6.16. (R)-3-Methoxy-4-(4-((1-phenylethyl)amino)thieno[2,3-d]pyrimidin-6-yl)benzaldehyde ((R)-**5s**)

Compound (*R*)-**5s** was prepared as described in Section 4.6.1, but starting with (4-formyl-2-methoxyphenyl)boronic acid (**4s**) (584 mg, 3.230 mmol). The reaction time was 9 h. Purification was by silica-gel column chromatography (*n*-pentane/Et_2O, 3/7), $R_f = 0.30$. This gave 0.891 mg (2.287 mmol, 84%) of (*R*)-**5s** as a bright yellow solid, mp 155–158 °C; HPLC purity: 99% (method A), $t_R = 30.5$ min; $[\alpha]_D^{20} = -486.3$ (*c* 0.98, DMSO); ^{1}H NMR (400 MHz, DMSO-d_6) δ: 10.03 (s, 1H), 8.47 (s, 1H), 8.34 (d, $J = 7.9$, 1H), 8.31 (s, 1H), 8.01–7.97 (m, 1H), 7.70–7.66 (m, 2H), 7.46–7.42 (m, 2H), 7.36–7.30 (m, 2H), 7.25–7.20 (m, 1H), 5.59–5.50 (m, 1H), 4.06 (s, 3H), 1.58 (d, $J = 7.1$, 3H); ^{13}C NMR (100 MHz, DMSO-d_6) δ: 192.2, 166.4, 155.8, 155.7, 154.2, 144.6, 136.6, 132.3, 128.3 (2C), 128.2, 127.6, 126.7, 126.1 (2C), 122.8, 119.4, 116.1, 112.2, 56.2, 49.0, 22.4; IR (neat, cm^{-1}): 3277, 3100, 2935, 2810, 1687, 1579, 1499, 1254, 1028, 735, 696, 559; HRMS (APCI/ASAP, *m/z*): 390.1274 (calcd. $C_{22}H_{20}N_3O_2S$, 390.1276, $[M + H]^+$).

*4.6.17. (R)-(3-Methoxy-4-(4-((1-phenylethyl)amino)thieno[2,3-d] pyrimidin-6-yl)phenyl)methanol ((R)-**5t**)*

Compound (*R*)-**5s** (285 mg, 0.733 mmol) was dissolved in MeOH (25 mL) and added $NaBH_4$ (30 mg, 0.793 mmol). The mixture was stirred for 10 min at 0 °C, before another portion of $NaBH_4$ (30 mg, 0.793 mmol) was added. The stirring was continued at rt for 2 h. The reaction mixture was then concentrated *in vacuo*, diluted with water (100 mL) and EtOAc (50 mL) and the water phase was extracted with EtOAc (2 × 50 mL). The combined organic phases were washed with saturated aq NaCl solution (30 mL), dried over anhydrous Na_2SO_4, filtered and concentrated *in vacuo*. The crude product was absorbed onto silica and purified by silica-gel column chromatography (Et_2O/EtOAc, 3/1), $R_f = 0.21$. Drying gave 194 mg (0.497 mmol, 68%) of (*R*)-**5t** as a white solid, mp 177–179 °C; HPLC purity: 98% (method A), $t_R = 26.6$ min; $[\alpha]_D^{20} = -377.3$ (*c* 1.04, DMSO); ^{1}H NMR (400 MHz, DMSO-d_6) δ: 8.26 (s, 1H), 8.22 (s, 1H), 8.19 (d, $J = 8.0$, 1H), 7.72–7.69 (m, 1H), 7.46–7.41 (m, 2H), 7.35–7.29 (m, 2H), 7.24–7.19 (m, 1H), 7.16–7.14 (m, 1H), 7.08–7.04 (m, 1H), 5.58–5.49 (m, 1H), 5.31 (t, $J = 5.8$, 1H), 4.56 (d, $J = 5.7$, 2H), 3.95 (s, 3H), 1.57 (d, $J = 7.1$, 3H); ^{13}C NMR (100 MHz, DMSO-d_6) δ: 165.5, 155.5, 155.4, 153.5, 144.8, 144.7, 134.1, 128.3 (2C), 127.6, 126.7, 126.1 (2C), 120.1, 118.9, 116.5, 116.2, 110.2, 62.6, 55.8, 48.9, 22.5; IR (neat, cm^{-1}): 3281, 2971, 2933, 2361, 1588, 1499, 1019, 767, 698; HRMS (APCI/ASAP, *m*/*z*): 392.1426 (calcd. $C_{22}H_{22}N_3O_2S$, 392.1433, $[M + H]^+$).

*4.6.18. (R)-N-(1-(4-Fluorophenyl)ethyl)-6-phenylthieno[2,3-d] pyrimidin-4-amine hydrochloride ((R)-**25a**·HCl)*

Compound **24a** (100 mg, 0.405 mmol) was mixed with (*R*)-1-(4-fluorophenyl)ethanamine ((*R*)-**6**) (0.16 mL, 168 mg, 1.21 mmol) and 1-butanol (2 mL), and agitated at 145 °C for 21 h. Then the mixture was cooled to rt, diluted with EtOAc (50 mL) and washed with water (3 × 15 mL). The combined organic phases were dried over anhydrous Na_2SO_4, filtered and concentrated *in vacuo*. The crude product was purified by silica-gel column chromatography (EtOAc), $R_f = 0.60$. The product was further purified by precipitation from diethyl ether (50 mL) by addition of HCl in diethyl ether (1.5 mL) and storage at −18 °C for 24 h. The solid was isolated by filtration and washed with diethyl ether (2 × 25 mL). Drying gave 108 mg (0.280 mmol, 69%) of (*R*)-**25a**·HCl as a white solid, mp 147–151 °C; HPLC purity: 95% (method B), $t_R = 18.6$ min; $[\alpha]_D^{20} = -268.0$ (*c* 1.02, DMSO); ^{1}H NMR (400 MHz, DMSO-d_6) δ: 8.29 (s, 1H), 8.24 (d, $J = 7.8$, 1H), 8.18 (s, 1H), 7.73–7.67 (m, 2H), 7.54–7.44 (m, 4H), 7.43–7.37 (m, 1H), 7.18–7.10 (m, 2H), 5.56–5.46 (m, 1H), 1.56 (d, $J = 7.0$, 3H); ^{13}C NMR (100 MHz, DMSO-d_6) δ: 165.1, 161.0 (d, $J = 242.2$), 155.7, 153.9, 140.8 (d, $J = 3.4$), 138.2, 133.2, 129.4 (2C), 128.6, 128.0 (d, $J = 8.1$, 2C), 125.7 (2C), 117.4, 115.5, 115.0 (d, $J = 21.1$, 2C), 48.5, 22.5; ^{19}F NMR (564 MHz, DMSO-d_6) δ: −118.6 (s); IR (neat, cm^{-1}): 3058, 2977, 1607, 1509, 1223, 838, 753, 688; HRMS (ESI, *m*/*z*): 350.1123 (calcd. $C_{20}H_{17}FN_3S$, 350.1122, $[M + H]^+$).

*4.6.19. (R)-6-(4-Fluorophenyl)-N-(1-(4-fluorophenyl)ethyl)thieno [2,3-d]pyrimidin-4-amine hydrochloride ((R)-**25c**·HCl)*

Compound (*R*)-**25c**·HCl was prepared as described in Section 4.6.18, but starting with compound **24c** (100 mg, 0.378 mmol). The crude product was purified by silica-gel column chromatography (*n*-pentane/acetone, 7/3), $R_f = 0.38$. The product was further purified by precipitation from diethyl ether (50 mL) by addition of HCl in diethyl ether (1.5 mL) and storage at −18 °C for 24 h. The solid was isolated by filtration and washed with diethyl ether (2 × 25 mL). Drying gave 106 mg (0.263 mmol, 70%) of (*R*)-**25c**·HCl as a white solid, mp 166–174 °C; HPLC purity: 97% (method B), $t_R = 19.4$ min; $[\alpha]_D^{20} = -244.8$ (*c* 0.92, DMSO); ^{1}H NMR (400 MHz, DMSO-d_6) δ: 8.29 (s, 1H), 8.25 (d, $J = 7.8$, 1H), 8.12 (s, 1H), 7.76–7.61 (m, 2H), 7.50–7.43 (m, 2H), 7.40–7.32 (m, 2H), 7.18–7.10 (m, 2H), 5.54–5.45 (m, 1H), 1.55 (d, $J = 7.0$, 3H); ^{13}C NMR (100 MHz, DMSO-d_6) δ: 165.2, 162.2 (d, $J = 246.3$), 161.1 (d, $J = 242.1$), 155.7, 153.9, 140.8 (d, $J = 2.9$), 137.1, 129.9 (d, $J = 3.3$), 128.0 (d, $J = 8.1$, 2C), 127.8 (d, $J = 8.3$, 2C), 117.5, 116.4 (d, $J = 22.0$, 2C), 115.7, 115.0 (d, $J = 21.2$, 2C), 48.5, 22.6; ^{19}F NMR (564 MHz, DMSO-d_6) δ: −115.3 (s), −118.6 (s); IR (neat, cm^{-1}): 3057, 2966, 2874, 1603, 1491, 1234, 832, 699; HRMS (ESI, *m*/*z*): 368.1029 (calcd. $C_{20}H_{16}F_2N_3S$, 368.1028, $[M + H]^+$).

*4.6.20. (R)-(4-(4-((1-(4-Fluorophenyl)ethyl)amino)thieno[2,3-d] pyrimidin-6-yl)phenyl)methanol ((R)-**25e**)*

The preparation of the 4-(hydroxymethyl)phenylboronic acid (**4e**) (140 mg, 0.920 mmol) and the cross-coupling reaction with the fluorinated compound (*R*)-**15**·HCl (200 mg, 0.515 mmol) were performed as described in Section 4.6.4. The reaction time was 2.5 h. The crude product was absorbed onto celite and purified by silica-gel column chromatography (EtOAc/*n*-pentane, 7/3), $R_f = 0.26$. Drying gave 77 mg (0.203 mmol, 39%) of (*R*)-**25e** as a white solid, mp 203–205 °C; HPLC purity: 98% (method A), $t_R = 27.2$ min; $[\alpha]_D^{20} = -265.7$ (*c* 1.17, DMSO); ^{1}H NMR (400 MHz, DMSO-d_6) δ: 8.28 (s, 1H), 8.22 (d, $J = 7.8$, 1H), 8.14 (s, 1H), 7.68–7.63 (m, 2H), 7.50–7.42 (m, 4H), 7.18–7.11 (m, 2H), 5.55–5.46 (m, 1H), 5.29 (t, $J = 5.7$, 1H), 4.55 (d, $J = 5.7$, 2H), 1.56 (d, $J = 7.0$, 3H); ^{13}C NMR (100 MHz, DMSO-d_6) δ: 165.4, 161.5 (d, $J = 241.7$), 156.1, 154.2, 143.7, 141.3 (d, $J = 3.1$), 138.8, 132.1, 128.5 (d, $J = 8.1$, 2C), 127.8 (2C), 125.9 (2C), 117.9, 115.50, 115.46 (d, $J = 21.2$, 2C), 62.9, 48.9, 23.0; ^{19}F NMR (564 MHz, DMSO-d_6) δ: −118.7 (s); IR (neat, cm^{-1}): 3242, 3131, 2924, 2854, 1578, 1510, 1312, 1227, 1099, 831, 801, 777; HRMS (APCI/ASAP, *m*/*z*): 380.1226 (calcd. $C_{21}H_{19}FN_3OS$, 380.1233, $[M + H]^+$).

*4.6.21. (R)-3-(4-(1-(4-Fluorophenyl)ethylamino)thieno[2,3-d] pyrimidin-6-yl)phenol hydrochloride ((R)-**25j**·HCl)*

Compound (*R*)-**25j**·HCl was prepared as described in Section 4.6.1, but starting with (3-hydroxyphenyl)boronic acid (**4j**) (115 mg, 0.834 mmol) and the fluorinated compound (*R*)-**15**·HCl (215 mg, 0.553 mmol). The reaction time was 3.5 h. The crude product was purified by silica-gel column chromatography (EtOAc), $R_f = 0.59$. The product was precipitated from *n*-pentane (100 mL) by addition of HCl in diethyl ether (2 mL) and storage at 4 °C for 4.5 h. Drying gave 213 mg (0.530 mmol, 96%) of (*R*)-**25j**·HCl as a white solid; mp 180–184 °C; HPLC purity: 98% (method C), $t_R = 15.7$ min; $[\alpha]_D^{20} = -282.7$ (*c* 1.00, DMSO); ^{1}H NMR (400 MHz, DMSO-d_6) δ: 9.73 (s, 1H), 8.28 (s, 1H), 8.22 (d, $J = 7.8$, 1H), 8.12 (s, 1H), 7.48–7.44 (m, 2H), 7.31–7.27 (m, 1H), 7.17–7.12 (m, 3H), 7.09–7.08 (m, 1H), 6.82–6.79 (m, 1H), 5.54–5.45 (m, 1H), 1.55 (d, $J = 7.0$, 3H); ^{13}C NMR (100 MHz, DMSO-d_6) δ: 165.0, 162.2 (d, $J = 240.8$), 158.0, 155.7, 153.8, 140.8 (d, $J = 3.0$), 138.4, 134.4, 130.5, 128.0 (d, $J = 8.0$, 2C), 117.4, 116.5, 115.7, 115.3, 115.1 (d, $J = 21.1$, 2C), 112.4, 48.5, 22.5; ^{19}F NMR (564 MHz, DMSO-d_6) δ: −118.7 (s); IR (neat, cm^{-1}): 3059, 2737, 2348, 1594, 1511, 1444, 1220, 763, 670, 571; HRMS (EI, 70 eV, *m*/*z*): 365.0995 (calcd. $C_{20}H_{16}ON_3FS$, 365.0993, $[M]^+$).

*4.6.22. (R)-(3-(4-(1-(4-Fluorophenyl)ethylamino)thieno[2,3-d] pyrimidin-6-yl)phenyl)methanol ((R)-**25l**)*

Compound (*R*)-**25l** was prepared as described in Section 4.6.1, but starting with (3-(hydroxymethyl)phenyl) boronic acid (**4l**) (149 mg, 0.981 mmol) and the fluorinated compound (*R*)-**15**·HCl (210 mg, 0.540 mmol). The crude product was purified by silica-gel column chromatography (EtOAc), $R_f = 0.52$. Further purification was done by crystallization from MeOH (1 mL) using water as anti-solvent (1 mL). This gave 143 mg (0.377 mmol, 70%) of (*R*)-**25l** as a slightly yellowish solid, mp 182–185 °C; HPLC purity: 98% (method C), $t_R = 14.9$ min; $[\alpha]_D^{20} = -324.9$ (*c* 0.93, DMSO); ^{1}H NMR (400 MHz, DMSO-d_6) δ: 8.29 (s, 1H), 8.26 (d, $J = 7.8$, 1H), 8.20 (s, 1H), 7.72 (s, 1H), 7.56–7.54 (m, 1H), 7.49–7.43 (m, 3H), 7.33–7.31 (m, 1H), 7.17–

7.12 (m, 2H), 5.55–5.46 (m, 1H), 5.34 (t, J = 5.7, 1H), 4.59 (d, J = 5.7, 2H), 1.56 (d, J = 7.0, 3H); ^{13}C NMR (100 MHz, DMSO-d_6) δ: 165.0, 162.2 (d, J = 240.8), 155.7, 153.9, 143.8, 140.8 (d, J = 3.0), 138.4, 133.0, 129.1, 128.0 (d, J = 8.1, 2C), 126.5, 124.0, 123.3, 117.5, 115.4, 115.1 (d, J = 21.1, 2C), 62.5, 48.5, 22.5; ^{19}F NMR (564 MHz, DMSO-d_6) δ: −118.7 (s); IR (neat, cm^{-1}): 3272, 2976, 2867, 1589, 1500, 1220, 1096, 774, 680, 566; HRMS (EI, 70 eV, m/z): 379.1149 (calcd. $C_{21}H_{18}FN_3OS$, 379.1149, $[M]^+$).

4.6.23. (R)-2-(4-(1-(4-Fluorophenyl)ethylamino)thieno[2,3-d]pyrimidin-6-yl)phenol ((R)-**25n**)

Compound (*R*)-**25n** was prepared as described in Section 4.6.1, but starting with (2-hydroxyphenyl)boronic acid (**4n**) (115 mg, 0.834 mmol) and the fluorinated compound (*R*)-**15**·HCl (212 mg, 0.545 mmol). The reaction time was 3 h. The crude product was purified by silica-gel column chromatography (EtOAc), R_f = 0.52. The product was precipitated from *n*-pentane (100 mL) by addition of HCl in diethyl ether (1 mL). This gave 156 mg (0.388 mmol, 71%) of a white powder with purity of 96% (HPLC). For further purification a fraction (82 mg, 0.204 mmol) was free-based and crystallized from MeOH (2 mL) using water as anti-solvent. This gave 55 mg (0.151 mmol, 67%) of (*R*)-**25n** as a white powder, mp 167–174 °C; HPLC purity: 98% (method C), t_R = 15.0 min; $[\alpha]_D^{20}$ = −347.3 (*c* 0.62, DMSO); ^{1}H NMR (400 MHz, DMSO-d_6) δ: 10.42 (s, 1H), 8.26 (s, 1H), 8.24–8.19 (m, 2H), 7.67–7.65 (m, 1H), 7.48–7.45 (m, 2H), 7.23–7.19 (m, 1H), 7.16–7.12 (m, 2H), 7.02–7.00 (m, 1H), 6.96–6.92 (m, 1H), 5.56–5.47 (m, 1H), 1.56 (d, J = 7.0, 3H); ^{13}C NMR (100 MHz, DMSO-d_6) δ: 165.4, 162.2 (d, J = 240.5), 155.5, 154.0, 153.3, 141.0 (d, J = 3.0), 135.0, 129.4, 128.0 (d, J = 8.0, 2C), 127.8, 120.1, 119.7, 116.5, 116.3, 116.2, 115.1 (d, J = 21.1, 2C), 48.4, 22.5; ^{19}F NMR (564 MHz, DMSO-d_6) δ: −118.8 (s); IR (neat, cm^{-1}): 2919, 1574, 1501, 1201, 737, 550; HRMS (EI, 70 eV, m/z): 365.0994 (calcd. $C_{20}H_{16}ON_3FS$, 365.0993, $[M]^+$).

4.6.24. (R)-N-(1-(4-Fluorophenyl)ethyl)-6-(2-methoxyphenyl)thieno[2,3-d]pyrimidin-4-amine ((R)-**25p**)

Compound (*R*)-**25p** was prepared as described in Section 4.6.1, but starting with (2-methoxyphenyl)boronic acid (**4p**) (119 mg, 0.785 mmol) and the fluorinated compound (*R*)-**15**·HCl (201 mg, 0.516 mmol). The reaction time was 3.5 h. The crude product was absorbed onto celite and purified by silica-gel column chromatography (*n*-pentane/EtOAc, 1/1), R_f = 0.43. Drying gave 163 mg (0.431 mmol, 83%) of (*R*)-**25p** as a white solid, mp 98–102 °C; HPLC purity: 98% (method A), t_R = 31.8 min; $[\alpha]_D^{20}$ = −296.0 (*c* 1.03, DMSO); ^{1}H NMR (400 MHz, DMSO-d_6) δ: 8.28 (s, 1H), 8.24–8.20 (m, 2H), 7.77–7.72 (m, 1H), 7.50–7.43 (m, 2H), 7.42–7.36 (m, 1H), 7.23–7.18 (m, 1H), 7.18–7.07 (m, 3H), 5.57–5.48 (m, 1H), 3.95 (s, 3H), 1.56 (d, J = 7.0, 3H); ^{13}C NMR (100 MHz, DMSO-d_6) δ: 165.6, 161.0 (d, J = 242.1), 155.53, 155.47, 153.6, 140.9 (d, J = 2.9), 134.0, 129.8, 128.0 (d, J = 8.2, 2C), 127.9, 121.8, 121.1, 117.0, 116.2, 115.0 (d, J = 21.2, 2C), 112.5, 55.9, 48.4, 22.5; ^{19}F NMR (564 MHz, DMSO-d_6) δ: −118.7 (s); IR (neat, cm^{-1}): 3242, 2971, 2836, 1577, 1506, 1221, 1115, 832, 747; HRMS (APCI/ASAP, m/z): 380.1230 (calcd. $C_{21}H_{19}FN_3OS$, 380.1233, $[M + H]^+$).

4.6.25. (R)-(2-(4-(1-(4-Fluorophenyl)ethylamino)thieno[2,3-d]pyrimidin-6-yl)phenyl)methanol ((R)-**25q**)

Compound (*R*)-**25q** was prepared as described in Section 4.6.1, but starting with (2-(hydroxymethyl)phenyl)boronic acid (**4q**) (85 mg, 0.559 mmol) and the fluorinated compound (*R*)-**15**·HCl (141 mg, 0.363 mmol). The reaction time was 4.5 h at 90 °C. The crude product was purified by silica-gel column chromatography (EtOAc), R_f = 0.46. This was followed by crystallization from MeOH (1.5 mL) using water as anti-solvent, which gave 108 mg (0.285 mmol, 80%) of (*R*)-**25q** as a white fluffy powder, mp 157–161 °C; HPLC purity 99% (method A), t_R = 24.4 min; $[\alpha]_D^{20}$ = −273.0 (*c* 1.01, DMSO); ^{1}H NMR (400 MHz, DMSO-d_6) δ: 8.31 (s, 1H), 8.25 (d, J = 7.8, 1H), 7.77 (s, 1H), 7.68–7.66 (m, 1H), 7.49–7.44 (m, 4H) 7.40–7.36 (m, 1H), 7.17–7.12 (m, 2H), 5.57–5.48 (m, 1H), 5.34 (t, J = 5.4, 1H), 4.68 (d, J = 5.4, 2H), 1.55 (d, J = 7.0, 3H); ^{13}C NMR (100 MHz, DMSO-d_6) δ: 166.1, 162.2 (d, J = 240.8), 155.8, 153.7, 140.8 (d, J = 3.0), 140.2, 136.5, 131.5, 130.0, 128.6, 128.0 (d, J = 8.0, 2C), 127.8, 127.2, 119.0, 116.8, 115.1 (d, J = 21.1, 2C), 60.9, 48.4, 22.5; ^{19}F NMR (564MHz, DMSO-d_6) δ: −118.7 (s); IR (neat, cm^{-1}): 3324, 2971, 2883, 1574, 1506, 1225, 1127, 763, 581; HRMS (EI, 70 eV, m/z): 379.1153 (calcd. $C_{21}H_{18}ON_3FS$, 379.1149, $[M]^+$).

4.6.26. 2-(4-(Benzylamino)thieno[2,3-d]pyrimidin-6-yl)phenol (**26n**)

Compound **26n** was prepared as described in Section 4.6.1, but starting with (2-hydroxyphenyl)boronic acid (**4n**) (90 mg, 0.653 mmol) and compound **16** (202 mg, 0.630 mmol). The reaction time was 2.5 h. The crude product was purified by silica-gel column chromatography (CH_2Cl_2/MeOH, 24/1), R_f = 0.15. Drying gave 43 mg (0.128 mmol, 20%) of **26n** as a white solid, mp 177–180 °C; HPLC purity: 97% (method A), t_R = 24.2 min; ^{1}H NMR (400 MHz, DMSO-d_6) δ: 10.42 (s, 1H), 8.50 (t, J = 5.9, 1H), 8.32 (s, 1H), 8.14 (s, 1H), 7.64–7.60 (m, 1H), 7.41–7.30 (m, 4H), 7.27–7.17 (m, 2H), 7.03–6.98 (m, 1H), 6.95–6.90 (m, 1H), 4.76 (d, J = 5.9, 2H); ^{13}C NMR (100 MHz, DMSO-d_6) δ: 165.2, 156.3, 154.0, 153.5, 139.6, 135.1, 129.3, 128.3 (2C), 127.8, 127.4 (2C), 126.8, 120.0, 119.7, 116.51, 116.46, 116.2, 43.3; IR (neat, cm^{-1}): 3422, 2922, 2852, 1578, 1454, 1348, 1107, 745; HRMS (APCI/ASAP, m/z): 334.1013 (calcd. $C_{19}H_{16}N_3OS$, 334.1014, $[M + H]^+$).

4.6.27. (R)-2-(4-((1-Phenylpropyl)amino)thieno[2,3-d]pyrimidin-6-yl)phenol ((R)-**27n**)

Compound (*R*)-**27n** was prepared as described in Section 4.6.1, but starting with (2-hydroxyphenyl)boronic acid (**4n**) (21 mg, 0.149 mmol) and compound (*R*)-**17** (37 mg, 0.096 mmol). The reaction time was 20 h. The crude product was absorbed onto celite and purified by silica-gel column chromatography (EtOAc/*n*-pentane, 3/2), R_f = 0.37. This gave 19 mg (0.053 mmol, 55%) of (*R*)-**27n** as a light brown solid, mp 167–171 °C; HPLC purity: 95% (method A), t_R = 29.3 min; $[\alpha]_D^{20}$ = −256.0 (*c* 0.42, DMSO-d_6); ^{1}H NMR (400 MHz, DMSO-d_6) δ: 10.24 (s, 1H), 8.26–8.24 (m, 2H), 8.15 (d, J = 8.3, 1H), 7.70–7.66 (m, 1H), 7.46–7.42 (m, 2H), 7.35–7.29 (m, 2H), 7.24–7.18 (m, 2H), 7.03–6.99 (m, 1H), 6.97–6.95 (m, 1H), 5.33–5.25 (m, 1H), 1.98–1.82 (m, 2H), 0.95 (t, J = 7.3, 3H); ^{13}C NMR (100 MHz, DMSO-d_6) δ: 165.4, 156.0, 153.9, 153.3, 143.9, 134.9, 129.3, 128.2 (2C), 127.8, 126.7, 126.6 (2C), 120.1, 119.6, 116.5, 116.3, 116.2, 55.3, 29.3, 11.5; IR (neat, cm^{-1}): 2923, 2853, 1578, 1451, 1354, 1294, 1105, 745, 697; HRMS (APCI/ASAP, m/z): 362.1324 (calcd. $C_{21}H_{20}N_3OS$, 362.1327, $[M + H]^+$).

4.6.28. (rac)-(4-((2-Methyl-1-phenylpropyl)amino)thieno[2,3-d]pyrimidin-6-yl)phenol ((rac)-**28n**)

Compound (*rac*)-**28n** was prepared as described in Section 4.6.1, but starting with compound (*rac*)-**18** (150 mg, 0.414 mmol) and (2-hydroxyphenyl)boronic acid (**4n**) (86 mg, 0.621 mmol) and reacting for 4 h. The crude product was purified with silica-gel column chromatography (CH_2Cl_2/MeOH, 49/1), R_f = 0.40, and then precipitated from diethyl ether (2 mL) and *n*-pentane (30 mL). Evaporation and drying gave 127 mg (0.339 mmol, 82%) of (*rac*)-**28n** as a white solid, mp 159–162 °C; HPLC purity: 96% (method A), t_R = 28.2 min; ^{1}H NMR (400 MHz, DMSO-d_6) δ: 10.41 (s, 1H), 8.25–8.24 (m, 2H), 8.11–8.07 (m, 1H), 7.71–7.67 (m, 1H), 7.47–7.45 (m, 2H), 7.34–7.31 (m, 2H), 7.23–7.19 (m, 2H), 7.01–6.93 (m, 2H), 5.12–5.07 (m, 1H), 2.27–2.15 (m, 1H), 1.07 (d, J = 6.6, 3H), 0.77 (d, J = 6.7, 3H); ^{13}C NMR (100 MHz, DMSO-d_6) δ: 165.4, 156.1, 153.9, 153.3,

143.0, 134.8, 129.3, 128.1 (2C), 127.8, 127.4 (2C), 126.7, 120.1, 119.6, 116.5, 116.1, 83.2, 60.2, 32.8, 20.1, 19.9; IR (neat, cm^{-1}): 3035, 2961, 1606, 1367, 758, 701; HRMS (APCI/ASAP, *m*/*z*): 376.1484 (calcd. $C_{22}H_{22}N_3OS$, 376.1484, $[M + H]^+$).

4.6.29. (*R*)-2-(4-(Methyl(1-phenylethyl)amino)thieno[2,3-d] pyrimidin-6-yl)phenol ((*R*)-**29n**)

Compound (*R*)-**29n** was prepared as described in Section 4.6.1, but starting with compound (*R*)-**19** (150 mg, 0.428 mmol) and (2-hydroxyphenyl)boronic acid (**4n**) (89 mg, 0.646 mmol), and reacting for 3.5 h. The crude product was purified with silica-gel column chromatography (*n*-pentane/EtOAc, 1/1), R_f = 0.43. The purified product was dissolved in diethyl ether (2 mL) and slowly added to *n*-pentane (30 mL) to give precipitation. Evaporation and drying gave 136 mg (0.378 mmol, 88%) of (*R*)-**29n** as a white solid, mp 227–230 °C; HPLC purity: 96% (method A), t_R = 28.1 min; $[\alpha]_D^{20} = -15.7$ (*c* 0.80, DMSO); ^{1}H NMR (400 MHz, DMSO-d_6) δ: 10.41 (s, 1H), 8.38 (s, 1H), 8.01 (s, 1H), 7.71–7.69 (m, 1H), 7.39–7.35 (m, 4H), 7.31–7.27 (m, 1H), 7.20–7.16 (m, 1H), 6.97–6.95 (m, 1H), 6.90–6.86 (m, 1H), 6.45–6.40 (m, 1H), 3.13 (s, 3H), 1.63 (d, J = 7.0, 3H); ^{13}C NMR (100 MHz, DMSO-d_6) δ: 168.3, 157.4, 154.1, 152.3, 141.1, 133.3, 129.3, 128.5 (2C), 128.2, 127.1, 126.9 (2C), 119.9, 119.6, 118.9, 116.3, 115.6, 53.4, 33.1, 16.3; IR (neat, cm^{-1}): 3052, 1589, 1380, 753, 699; HRMS (APCI/ASAP, *m*/*z*): 362.1322 (calcd. $C_{21}H_{20}N_3OS$, 362.1327, $[M + H]^+$).

4.6.30. (*rac*)-2-(4-((2,2,2-Trifluoro-1-phenylethyl)amino)thieno [2,3-d]pyrimidin-6-yl)phenol ((*rac*)-**30n**)

Compound (*rac*)-**30n** was prepared as described in Section 4.6.1, but starting with compound (*rac*)-**20**·HCl (221 mg, 0.521 mmol) and (2-hydroxyphenyl)boronic acid (**4n**) (108 mg, 0.781 mmol), and reacting for 3.5 h. The crude product was purified with silica-gel column chromatography (diethyl ether), R_f = 0.48. The purified product was dissolved in diethyl ether (2 mL), slowly added to *n*-pentane (30 mL) to give precipitation. Isolation and drying gave 162 mg (0.403 mmol, 85%) of (*rac*)-**30n** as a white solid, mp 236 °C (dec.); HPLC purity: 97% (method A), t_R = 30.5 min; ^{1}H NMR (400 MHz, DMSO-d_6) δ: 10.59 (br s, 1H), 8.85 (d, J = 9.5, 1H), 8.47–8.45 (m, 2H), 7.75–7.71 (m, 3H), 7.49–7.40 (m, 3H), 7.26–7.22 (m, 1H), 7.05–7.03 (m, 1H), 6.98–6.94 (m, 1H), 6.63–6.54 (m, 1H); ^{13}C NMR (100 MHz, DMSO-d_6) δ: 166.9, 155.7, 154.5, 153.2, 136.5 (2C), 133.9, 130.1, 129.5, 129.1 (2C), 129.0 (2C), 128.3, 125.6 (q, J = 282.7), 120.3, 120.1, 117.0, 116.5, 54.5 (q, J = 22.9); ^{19}F NMR (564 MHz, DMSO-d_6) δ: −74.1 (s); IR (neat, cm^{-1}): 3313, 2983, 1546, 1072, 654; HRMS (EI, 70 eV, *m*/*z*): 401.0805, (calcd. $C_{20}H_{14}F_3N_3OS$, 401.0804, $[M]^+$).

4.6.31. (*rac*)-2-(4-((2–Fluoro-1-phenylethyl)amino)thieno[2,3-d] pyrimidin-6-yl)phenol ((*rac*)-**31n**)

Compound (*rac*)-**31n** was prepared as described in Section 4.6.1, but starting with compound (*rac*)-**21** (150 mg, 0.42 mmol) and (2-hydroxyphenyl)boronic acid (**4n**) (88 mg, 0.639 mmol). The reaction was then stirred at 50 °C for 72 h under N_2 atmosphere. The crude product was purified with silica-gel column chromatography (*n*-pentane/EtOAc, 1/1), R_f = 0.43. The purified product was dissolved in diethyl ether (2 mL) and slowly added to *n*-pentane (30 mL) to give precipitation. Evaporation and drying gave 79 mg (0.216 mmol, 51%) of (*rac*)-**31n** as a white solid, mp 176–179 °C; HPLC purity: 96% (method A), t_R = 24.2 min; ^{1}H NMR (400 MHz, DMSO-d_6) δ: 10.49 (s, 1H), 8.46–8.44 (m, 1H), 8.29–8.27 (m, 2H), 7.69–7.67 (m, 1H), 7.52–7.50 (m, 2H), 7.39–7.35 (m, 2H), 7.31–7.27 (m, 1H), 7.24–7.20 (m, 1H), 7.03–7.01 (m, 1H), 6.96–6.93 (m, 1H), 5.87–5.78 (m, 1H), 4.87–4.80 (m, 1H), 4.75–4.69 (m, 1H); ^{13}C NMR (100 MHz, DMSO-d_6) δ: 165.5, 155.9, 154.1, 153.2, 138.4 (d, J = 6.0), 135.4, 129.4, 128.4 (2C), 127.9, 127.5, 127.2 (2C), 120.0, 119.6, 116.54, 116.50, 116.0, 84.3 (d, J = 174.9), 53.7 (d, J = 20.2); ^{19}F NMR (564 MHz, DMSO-d_6) δ: −219.7 (s); IR (neat, cm^{-1}): 3029, 2696, 1738, 1580, 1451, 1217, 749, 693; HRMS (APCI/ASAP, *m*/*z*): 366.1075 (calcd. $C_{20}H_{17}FN_3OS$, 366.1075, $[M + H]^+$).

4.6.32. (*S*)-2-(4-((2-Methoxy-1-phenylethyl)amino)thieno[2,3-d] pyrimidin-6-yl)phenol ((*S*)-**32n**)

Compound (*S*)-**32n** was prepared as described in Section 4.6.1, but starting with compound (*S*)-**22** (130 mg, 0.357 mmol) and (2-hydroxyphenyl)boronic acid (**4n**) (74 mg, 0.537 mmol), and reacting for 5 h. The crude product was purified with silica-gel column chromatography (*n*-pentane/EtOAc, 1/1), R_f = 0.48. The purified product was dissolved in diethyl ether (2 mL) and slowly added to *n*-pentane (30 mL) to give precipitation. Evaporation and drying gave 113 mg (0.299 mmol, 84%) of (*S*)-**32n** as a white solid, mp 221–224 °C; HPLC purity (method A): 97%, t_R = 26.8 min; $[\alpha]_D^{20} = -282.3$ (*c* 0.67, DMSO); ^{1}H NMR (400 MHz, DMSO-d_6) δ: 10.44 (s, 1H), 8.27–8.25 (m, 3H), 7.69–7.67 (m, 1H), 7.48–7.46 (m, 2H), 7.35–7.32 (m, 2H), 7.26–7.20 (m, 2H), 7.02–7.00 (m, 1H), 6.96–6.93 (m, 1H), 5.71–5.65 (m, 1H), 3.78 (dd_{AB}, J = 10.1, 8.8, 1H), 3.65 (dd_{AB}, J = 10.1, 5.2, 1H), 3.32 (s, 3H); ^{13}C NMR (100 MHz, DMSO-d_6) δ: 165.9, 156.4, 154.4, 153.8, 141.1, 135.5, 129.8, 128.7 (2C), 128.3, 127.6, 127.5 (2C), 120.5, 120.1, 117.0, 116.9, 116.7, 75.2, 58.5, 53.5; IR (neat, cm^{-1}): 3439, 2887, 1580, 1106, 745, 689; HRMS (APCI/ASAP, *m*/*z*): 378.1276 (calcd. $C_{21}H_{20}N_3O_2S$, 378.1276, $[M + H]^+$).

4.6.33. (*R*)-2-(4-((2-Methoxy-1-phenylethyl)amino)thieno[2,3-d] pyrimidin-6-yl)phenol ((*R*)-**32n**)

Compound (*R*)-**32n** was prepared as described in Section 4.6.1, but starting with compound (*R*)-**22**·HCl (150 mg, 0.374 mmol) and (2-hydroxyphenyl)boronic acid (**4n**) (77 mg, 0.558 mmol), and reacting for 4 h. The crude product was purified by silica-gel column chromatography (*n*-pentane/EtOAc, 1/1), R_f = 0.46. The purified product was dissolved in diethyl ether (2 mL) and slowly added to *n*-pentane (30 mL) to give precipitation. Evaporation and drying gave 130 mg (0.344 mmol, 92%) of (*R*)-**32n** as a white solid, mp 219–222 °C; HPLC purity: 96% (method A), t_R = 26.7 min; $[\alpha]_D^{20} = 263.3$ (*c* 0.76, DMSO); ^{1}H NMR (400 MHz, DMSO-d_6) δ: 10.45 (s, 1H), 8.27–8.24 (m, 3H), 7.69–7.67 (m, 1H), 7.48–7.46 (m, 2H), 7.35–7.31 (m, 2H), 7.26–7.21 (m, 2H), 7.02–7.00 (m, 1H), 6.96–6.93 (m, 1H), 5.71–5.65 (m, 1H), 3.81–3.76 (m, 1H), 3.67–3.63 (m, 1H), 3.32 (s, 3H); HRMS (APCI/ASAP, *m*/*z*): 378.1277 (calcd. $C_{21}H_{20}N_3O_2S$, 378.1276, $[M + H]^+$). The spectroscopic properties confirmed with that reported for (*S*)-**32n**.

4.6.34. (*S*)-2-((6-(4-(Hydroxymethyl)phenyl)thieno[2,3-d] pyrimidin-4-yl)amino)-2-phenylethan-1-ol ((*S*)-**33e**)

Compound (*S*)-**33e** was prepared as described in Section 4.6.1, but starting with compound (*S*)-**23**·HCl (150 mg, 0.388 mmol) and (4-(hydroxymethyl)phenyl)boronic acid (**4e**) (88 mg, 0.579 mmol), and reacting for 4 h. The crude product was purified by silica-gel column chromatography (EtOAc), R_f = 0.18. The purified product was dissolved in diethyl ether (2 mL) and slowly added to *n*-pentane (30 mL) to give precipitation. Evaporation and drying gave 123 mg (0.326 mmol, 84%) of (*S*)-**33e** as a white solid, mp 206–209 °C; HPLC purity: 96% (method A), t_R = 19.3 min; $[\alpha]_D^{20} = -309.3$ (*c* 0.63, DMSO); ^{1}H NMR (400 MHz, DMSO-d_6) δ: 8.27 (s, 1H), 8.24 (s, 1H), 8.19–8.17 (m, 1H), 7.69–7.67 (m, 2H), 7.46–7.44 (m, 4H), 7.34–7.31 (m, 2H), 7.26–7.21 (m, 1H), 5.48–5.43 (m, 1H), 5.30–5.28 (m, 1H), 5.06–5.03 (m, 1H), 4.56–4.55 (m, 2H), 3.82–3.72 (m, 2H); ^{13}C NMR (100 MHz, DMSO-d_6) δ: 165.4, 156.9, 154.2, 143.6, 141.5, 138.6, 134.1, 128.6 (2C), 127.8 (2C), 127.5 (2C), 127.4, 125.8 (2C), 118.1, 115.7, 65.2, 62.9, 56.8; IR (neat, cm^{-1}): 3326, 3261, 1595, 1316, 1041, 699; HRMS (APCI/ASAP, *m*/*z*): 378.1276 (calcd. $C_{21}H_{20}N_3O_2S$, 378.1276, $[M + H]^+$).

*4.6.35. (S)-2-(4-((2-Hydroxy-1-phenylethyl)amino)thieno[2,3-d] pyrimidin-6-yl)phenol ((S)-**33n**)*

Compound (*S*)-**33n** was prepared as described in Section 4.6.1, but starting with compound (*S*)-**23**·HCl (150 mg, 0.388 mmol) and (2-hydroxyphenyl)boronic acid (**4n**) (80 mg, 0.580 mmol), and reacting for 3 h. The crude product was purified with silica-gel column chromatography (EtOAc), $R_f = 0.30$. The purified product was dissolved in diethyl ether (2 mL) and slowly added to *n*-pentane (30 mL) to give precipitation. Evaporation and drying gave 116 mg (0.319 mmol, 82%) of (*S*)-**33n** as a white solid, mp 137–139 °C; HPLC purity: 97% (method A), $t_R = 23.5$ min; $[\alpha]_D^{20} = -293.3$ (*c* 0.84, DMSO); ^{1}H NMR (400 MHz, DMSO-d_6) δ: 10.43 (s, 1H), 8.28 (s, 1H), 8.24 (s, 1H), 8.18–8.16 (m, 1H), 7.70–7.68 (m, 1H), 7.45–7.43 (m, 2H), 7.34–7.30 (m, 2H), 7.24–7.19 (m, 2H), 7.02–7.00 (m, 1H), 6.96–6.93 (m, 1H), 5.49–5.42 (m, 1H), 5.04–5.01 (m, 1H), 3.83–3.72 (m, 2H); ^{13}C NMR (100 MHz, DMSO-d_6) δ: 165.8, 156.6, 154.4, 153.8, 141.7, 135.3, 129.8, 128.6 (2C), 128.3, 127.5 (2C), 127.3, 120.6, 120.1, 117.0, 116.9, 116.8, 65.2, 60.2; IR (neat, cm^{-1}): 3057, 1578, 1450, 747, 698; HRMS (APCI/ASAP, *m*/*z*): 364.118 (calcd. $C_{20}H_{18}N_3O_2S$, 364.1120, $[M + H]^+$).

*4.6.36. (R)-2-(4-((2-Hydroxy-1-phenylethyl)amino)thieno[2,3-d] pyrimidin-6-yl)phenol ((R)-**33n**)*

Compound (*R*)-**33n** was prepared as described in Section 4.6.1, but starting with compound (*R*)-**23** (150 mg, 0.428 mmol) and (2-hydroxyphenyl)boronic acid (**4n**) (89 mg, 0.645 mmol), and reacting for 6 h. The crude product was purified by silica-gel column chromatography (EtOAc), $R_f = 0.32$. The purified product was dissolved in diethyl ether (2 mL) and slowly added to *n*-pentane (30 mL) to give precipitation. Evaporation and drying gave 124 mg (0.341 mmol, 80%) of (*R*)-**33n** as a white solid, mp 136–139 °C; HPLC purity: 97% (method A), $t_R = 23.5$ min; $[\alpha]_D^{20} = 275.2$ (*c* 0.58, DMSO); ^{1}H NMR (400 MHz, DMSO-d_6) δ: 10.44 (s, 1H), 8.28 (s, 1H), 8.24 (s, 1H), 8.18–8.16 (m, 1H), 7.70–7.68 (m, 1H), 7.45–7.43 (m, 2H), 7.34–7.30 (m, 2H), 7.24–7.19 (m, 2H), 7.02–7.00 (m, 1H), 6.96–6.93 (m, 1H), 5.49–5.42 (m, 1H), 5.04–5.01 (m, 1H), 3.83–3.72 (m, 2H); HRMS (APCI/ASAP, *m*/*z*): 364.1119 (calcd. $C_{20}H_{18}N_3O_2S$, 364.1120, $[M + H]^+$). The spectroscopic properties confirmed with that reported for (*S*)-**33n**.

*4.6.37. (S)-2-((6-(2-Methoxyphenyl)thieno[2,3-d]pyrimidin-4-yl) amino)-2-phenylethan-1-ol ((S)-**33p**)*

Compound (*S*)-**33p** was prepared as described in Section 4.6.1, but with starting compound (*S*)-**23**·HCl (150 mg, 0.388 mmol) and (2-methoxyphenyl)boronic acid (**4p**) (88 mg, 0.579 mmol), reacting for 4 h. The crude product was purified by silica-gel column chromatography (*n*-pentane/EtOAc, 2/8), $R_f = 0.29$. The purified product was dissolved in diethyl ether (2 mL) and slowly added to *n*-pentane (30 mL) to give precipitation. Evaporation and drying gave 130 mg (0.344 mmol, 89%) of (*S*)-**33p** as a white solid, mp 186–189 °C; HPLC purity: 98% (method A), $t_R = 23.7$ min; $[\alpha]_D^{20} = -307.8$ (*c* 0.70, DMSO); ^{1}H NMR (400 MHz, DMSO-d_6) δ: 8.28–8.26 (m, 2H), 8.18–8.16 (m, 1H), 7.78–7.76 (m, 1H), 7.45–7.37 (m, 3H), 7.34–7.30 (m, 2H), 7.25–7.19 (m, 2H), 7.13–7.09 (m, 1H), 5.50–5.45 (m, 1H), 5.06–5.03 (m, 1H), 3.96 (s, 3H), 3.83–3.73 (m, 2H); ^{13}C NMR (100 MHz, DMSO-d_6) δ: 166.1, 156.7, 155.9, 154.0, 141.6, 134.3, 130.2, 128.6 (2C), 128.4, 127.5 (2C), 127.3, 122.3, 121.6, 117.5, 116.8, 113.0, 65.1, 56.8, 56.3; IR (neat, cm^{-1}): 3274, 3085, 2836, 1582, 1509, 1024, 747, 697; HRMS (APCI/ASAP, *m*/*z*): 378.1274 (calcd. $C_{21}H_{20}N_3O_2S$, 378.1276, $[M + H]^+$).

*4.6.38. (S)-4-(4-((2-Hydroxy-1-phenylethyl)amino)thieno[2,3-d] pyrimidin-6-yl)-3-methoxybenzaldehyde ((S)-**33s**)*

Compound (*S*)-**33s** was prepared as described in Section 4.6.1, but starting with (4-formyl-2-methoxyphenyl)boronic acid (**4s**) (168 mg, 0.931 mmol) and the building block (*S*)-**23**·HCl (307 mg, 0.778 mmol). The reaction time was 3 h. The crude product was purified by silica gel column chromatography (EtOAc/*n*-pentane, 9/1), $R_f = 0.27$. This gave 225 mg (0.554 mmol, 71%) of (*S*)-**33s** as a bright yellow solid, mp 203–206 °C; HPLC purity: 96% (method A), $t_R = 22.6$ min; $[\alpha]_D^{20} = -249.8$ (*c* 0.92, DMSO); ^{1}H NMR (400 MHz, DMSO-d_6) δ: 10.04 (s, 1H), 8.52 (s, 1H), 8.33–8.27 (m, 2H), 8.04–7.99 (m, 1H), 7.71–7.66 (m, 2H), 7.48–7.42 (m, 2H), 7.37–7.29 (m, 2H), 7.27–7.20 (m, 1H), 5.53–5.43 (m, 1H), 5.06 (t, $J = 5.6$, 1H), 4.07 (s, 3H), 3.83–3.73 (m, 2H); ^{13}C NMR (100 MHz, DMSO-d_6) δ: 192.2, 166.3, 156.5, 155.7, 154.2, 141.0, 136.6, 132.3, 128.20 (2C), 128.18, 127.6, 127.0 (2C), 126.9, 122.8, 119.5, 116.2, 112.2, 64.6, 56.4, 56.2; IR (neat, cm^{-1}): 3270, 3064, 2837, 1693, 1592, 1509, 1266, 1154, 1030, 773, 696, 562; HRMS (APCI/ASAP, *m*/*z*): 406.1222 (calcd. $C_{22}H_{20}N_3O_3S$, 406.1225, $[M + H]^+$).

*4.6.39. (S)-2-((6-(4-(Hydroxymethyl)-2-methoxyphenyl)thieno [2,3-d]pyrimidin-4-yl)amino)-2-phenylethanol ((S)-**33t**)*

Compound (*S*)-**33t** was prepared as described in Section 4.6.17, but starting with compound (*S*)-**33s** (71 mg, 0.174 mmol). The crude product was purified by silica-gel column chromatography (EtOAc), $R_f = 0.20$. Drying gave 33 mg (0.081 mmol, 47%) of (*S*)-**33t** as a pale yellow solid, mp 183–185 °C; HPLC purity: 96% (method A): $t_R = 18.8$ min; $[\alpha]_D^{20} = -332.0$ (*c* 1.00, DMSO); ^{1}H NMR (400 MHz, DMSO-d_6) δ: 8.27–8.24 (m, 2H), 8.15 (d, $J = 8.0$, 1H), 7.75–7.71 (m, 1H), 7.46–7.42 (m, 2H), 7.35–7.29 (m, 2H), 7.26–7.20 (m, 1H), 7.17–7.15 (m, 1H), 7.09–7.04 (m, 1H), 5.50–5.43 (m, 1H), 5.32 (t, $J = 5.7$, 1H), 5.03 (t, $J = 5.7$, 1H), 4.56 (d, $J = 5.7$, 2H), 3.95 (s, 3H), 3.83–3.72 (m, 2H); ^{13}C NMR (100 MHz, DMSO-d_6) δ: 165.5, 156.2, 155.4, 153.5, 144.8, 141.2, 134.0, 128.2 (2C), 127.6, 127.0 (2C), 126.9, 120.2, 118.9, 116.5, 116.3, 110.2, 64.7, 62.6, 56.3, 55.8; IR (neat, cm^{-1}): 3267, 3027, 2834, 1595, 1509, 1049, 772, 692, 559; HRMS (APCI/ASAP, *m*/*z*): 408.1380 (calcd. $C_{22}H_{22}N_3O_3S$, 408.1382, $[M + H]^+$).

Author contributions

Cellular experiments were performed by Unni Nonstad and Geir Bjørkøy. The synthetic work was performed by Steffen Bugge, Svein Jacob Kaspersen and Synne Larsen. Docking experiments were performed by Eirik Sundby.

Acknowledgements

Susana Villa Gonzalez is acknowledged for the HRMS experiments. Roger Aarvik, Jin Han and Ellen M. Skjønsfjell are acknowledged for their contributions. Prof. Dr. Justus Duyster and Dr. Nikolas von Bubnoff, Technical University of Munich, Munich, Germany kindly provided EGFR Ba/F3 cells. Anders Jahres Foundation and Technology Transfer Office (TTO-NTNU Trondheim) are thanked for financial support.

Appendix A. Supporting information

Supplementary data related to this article can be found at http://dx.doi.org/10.1016/j.ejmech.2014.01.042.

References

[1] M.K. Nedergaard, C.J. Hedegaard, H.S. Poulsen, Targeting the epidermal growth factor receptor in solid tumor malignancies, BioDrugs 26 (2012) 83–99.
[2] R. Patel, H.Y. Leung, Targeting the EGFR-family for therapy: biological challenges and clinical perspective, Curr. Pharm. Des. 18 (2012) 2672–2679.
[3] P. Warnault, A. Yasri, M. Coisy-Quivy, G. Cheve, C. Bories, B. Fauvel, R. Benhida, Recent advances in drug design of epidermal growth receptor inhibitors, Curr. Med. Chem. 20 (2013) 2043–2067.

[4] S. Li, K.R. Schmitz, P.D. Jeffrey, J.J.W. Wiltzius, P. Kussie, K.M. Ferguson, Structural basis for inhibition of the epidermal growth factor receptor by cetuximab, Cancer Cell 7 (2005) 301–311.

[5] X.D. Yang, X.C. Jia, J.R.F. Corvalan, P. Wang, C.G. Davis, A. Jakobovits, Eradication of established tumors by a fully human monoclonal antibody to the epidermal growth factor receptor without concomitant chemotherapy, Cancer Res. 59 (1999) 1236–1243.

[6] J. Kurai, H. Chikumi, K. Hashimoto, K. Yamaguchi, A. Yamasaki, T. Sako, H. Touge, H. Makino, M. Takata, M. Miyata, M. Nakamoto, N. Burioka, E. Shimizu, Antibody-dependent cellular cytotoxicity mediated by cetuximab against lung cancer cell lines, Clin. Cancer Res. 13 (2007) 1552–1561.

[7] W. Han, H.W. Lo, Landscape of EGFR signaling network in human cancers: biology and therapeutic response in relation to receptor subcellular locations, Cancer Lett. 318 (2012) 124–134.

[8] J. Stamos, M.X. Sliwkowski, C. Eigenbrot, Structure of the epidermal growth factor receptor kinase domain alone and in complex with a 4-anilinoquinazoline inhibitor, J. Biol. Chem. 277 (2002) 46265–46272.

[9] E.R. Wood, A.T. Truesdale, O.B. McDonald, D. Yuan, A. Hassell, S.H. Dickerson, B. Ellis, C. Pennisi, E. Horne, K. Lackey, K.J. Alligood, D.W. Rusnak, T.M. Gilmer, L. Shewchuk, A unique structure for epidermal growth factor receptor bound to GW572016 (Lapatinib): relationships among protein conformation, inhibitor off-rate, and receptor activity in tumor cells, Cancer Res. 64 (2004) 6652–6659.

[10] C.H. Yun, T.J. Boggon, Y. Li, M.S. Woo, H. Greulich, M. Meyerson, M.J. Eck, Structures of lung cancer-derived EGFR mutants and inhibitor complexes: mechanism of activation and insights into differential inhibitor sensitivity, Cancer Cell 11 (2007) 217–227.

[11] J.H. Park, Y. Liu, M.A. Lemmon, R. Radhakrishnan, Erlotinib binds both inactive and active conformations of the EGFR tyrosine kinase domain, Biochem. J. 448 (2012) 417–423.

[12] S.J. Kaspersen, C. Sørum, V. Willassen, E. Fuglseth, E. Kjøbli, G. Bjørkøy, E. Sundby, B.H. Hoff, Synthesis and *in vitro* EGFR (ErbB1) tyrosine kinase inhibitory activity of 4-*N*-substituted 6-aryl-7*H*-pyrrolo[2,3-*d*]pyrimidine-4-amines, Eur. J. Med. Chem. 46 (2011) 6002–6014.

[13] G. Varvounis, T. Giannopoulos, Synthesis, chemistry, and biological properties of thienopyrimidines, Adv. Heterocycl. Chem. 66 (1996) 193–283.

[14] V.P. Litvinov, The chemistry of thienopyrimidines, Adv. Heterocycl. Chem. 92 (2006) 83–143.

[15] N. Umeda, M. Takada, S. Ikeyama, K. Ichikawa, Preparation of Thienopyrimidine Derivatives as cGMP-specific Phosphodiesterase Inhibitors, WO 2002026745 A1, 4-4-2002.

[16] S. De Jonghe, L.-J. Gao, P. Herdewijn, J. Herman, M. Jang, P. Leyssen, T. Louat, J. Neyts, C. Pannecouque, B. Vanderhoydonck, Preparation of Bicyclic Heterocycles as Antiviral Agents, WO 2011147753 A1, 1-12-2011.

[17] H.-P. Hsieh, S.M. Coumar, T.-A. Hsu, W.-H. Lin, Y.-R. Chen, Y.-S. Chao, Preparation of Fused Bicyclic and Tricyclic Pyrimidine Compounds as Tyrosine Kinase Inhibitors, US 20100120805 A1, 13-5-2010.

[18] S. Jaekel, S. Murfin, S. Taylor, B. Aicher, A.-R. Kelter, T. Coulter, Thienopyrimidines for Pharmaceutical Compositions and their Preparation and use as Kinase Inhibitors, WO 2006136402 A1, 28-12-2006.

[19] M.J. Munchhof, J.S. Beebe, J.M. Casavant, B.A. Cooper, J.L. Doty, R.C. Higdon, S.M. Hillerman, C.I. Soderstrom, E.A. Knauth, M.A. Marx, A.M. Rossi, S.B. Sobolov, J. Sun, Design and SAR of thienopyrimidine and thienopyridine inhibitors of VEGFR-2 kinase activity, Bioorg. Med. Chem. Lett. 14 (2004) 21–24.

[20] M.J. Munchhof, S.B. Sobolov-Jaynes, M.A. Marx, Preparation of Thienopyrimidines and Thienopyridines as Anticancer Agents, US 6492383 B1, 10-12-2002.

[21] T.R. Rheault, T.R. Caferro, S.H. Dickerson, K.H. Donaldson, M.D. Gaul, A.S. Goetz, R.J. Mullin, O.B. McDonald, K.G. Petrov, D.W. Rusnak, L.M. Shewchuk, G.M. Spehar, A.T. Truesdale, D.E. Vanderwall, E.R. Wood, D.E. Uehling, Thienopyrimidine-based dual EGFR/ErbB-2 inhibitors, Bioorg. Med. Chem. Lett. 19 (2009) 817–820.

[22] T. Beckers, A. Sellmer, E. Eichhorn, H. Pongratz, C. Schaechtele, F. Totzke, G. Kelter, R. Krumbach, H.H. Fiebig, F.D. Boehmer, S. Mahboobi, Novel inhibitors of epidermal growth factor receptor: (4-(arylamino)-7*H*-pyrrolo[2,3-*d*]pyrimidin-6-yl)(1*H*-indol-2-yl)methanones and (1*H*-indol-2-yl)(4-(phenylamino)thieno[2,3-*d*]pyrimidin-6-yl)methanones, Bioorg. Med. Chem. 20 (2012) 125–136.

[23] C.H. Wu, M.S. Coumar, C.Y. Chu, W.H. Lin, Y.R. Chen, C.T. Chen, H.Y. Shiao, S. Rafi, S.Y. Wang, H. Hsu, C.H. Chen, C.Y. Chang, T.Y. Chang, T.W. Lien, M.Y. Fang, K.C. Yeh, C.P. Chen, T.K. Yeh, S.H. Hsieh, J.T.A. Hsu, C.C. Liao, Y.S. Chao, H.P. Hsieh, Design and synthesis of tetrahydropyridothieno[2,3-*d*]pyrimidine scaffold based epidermal growth factor receptor (EGFR) kinase inhibitors: the role of side chain chirality and Michael acceptor group for maximal potency, J. Med. Chem. 53 (2010) 7316–7326.

[24] G. Caravatti, J. Bruggen, E. Buchdunger, R. Cozens, P. Furet, N. Lydon, T. O'Reilly, P. Traxler, Pyrrolo[2,3-*d*]pyrimidine and pyrazolo[3,4-*d*]pyrimidine derivatives as selective inhibitors of the EGF receptor tyrosine kinase, ACS Symp. Ser. 796 (2001) 231–244.

[25] S. Bugge, S.J. Kaspersen, E. Sundby, B.H. Hoff, Route selection in the synthesis of C-4 and C-6 substituted thienopyrimidines, Tetrahedron 68 (2012) 9226–9233.

[26] C. Laurence, K.A. Brameld, J. Graton, J.Y. Le Questel, E. Renault, The pKBHX database: toward a better understanding of hydrogen-bond basicity for medicinal chemists, J. Med. Chem. 52 (2009) 4073–4086.

[27] C. Hansch, A. Leo, D. Hoekman, Exploring QSAR.Hydrophobic, Electronic and Steric Constants, in: ACS Professional Reference Book, American Chemical Society, Washington, DC, 1995.

[28] F. Leroux, Atropisomerism, biphenyls, and fluorine: a comparison of rotational barriers and twist angles, ChemBioChem 5 (2004) 644–649.

[29] Y.H. Peng, H.Y. Shiao, C.H. Tu, P.M. Liu, J.T.-A. Hsu, P.K. Amancha, J.S. Wu, M.S. Coumar, C.H. Chen, S.Y. Wang, W.H. Lin, H.Y. Sun, Y.S. Chao, P.C. Lyu, H.P. Hsieh, S.Y. Wu, Protein kinase inhibitor design by targeting the Asp-Phe-Gly (DFG) motif: the role of the DFG motif in the design of epidermal growth factor receptor inhibitors, J. Med. Chem. 56 (2013) 3889–3903.

[30] W.K. Hagmann, The many roles for fluorine in medicinal chemistry, J. Med. Chem. 51 (2008) 4359–4369.

[31] H.J. Boehm, D. Banner, S. Bendels, M. Kansy, B. Kuhn, K. Mueller, U. Obst-Sander, M. Stahl, Fluorine in medicinal chemistry, ChemBioChem 5 (2004) 637–643.

[32] G.W. Rewcastle, W.A. Denny, A.J. Bridges, H. Zhou, D.R. Cody, A. McMichael, D.W. Fry, Tyrosine kinase inhibitors. 5. Synthesis and structure–activity relationships for 4-[(phenylmethyl)amino]- and 4-(phenylamino)quinazolines as potent adenosine 5′-triphosphate binding site inhibitors of the tyrosine kinase domain of the epidermal growth factor receptor, J. Med. Chem. 38 (1995) 3482–3487.

[33] P.P. Graczyk, Gini coefficient: a new way to express selectivity of kinase inhibitors against a family of kinases, J. Med. Chem. 50 (2007) 5773–5779.

[34] J.L. Dargart, K. Fish, L.I. Gordon, R. Longnecker, O. Cen, Dasatinib therapy results in decreased B cell proliferation, splenomegaly, and tumor growth in a murine model of lymphoma expressing Myc and Epstein-Barr virus LMP2A, Antivir. Res. 95 (2012) 49–56.

[35] F. Frezzato, C. Gattazzo, V. Martini, V. Trimarco, A. Teramo, S. Carraro, A. Cabrelle, E. Ave, M. Facco, R. Zambello, E. Tibaldi, A.M. Brunati, G. Semenzato, L. Trentin, HS1, a Lyn kinase substrate, is abnormally expressed in B-chronic lymphocytic leukemia and correlates with response to fludarabine-based regimen, PLoS One 7 (2012) e39902.

[36] V.H. Duong, M.V. Jaglal, L. Zhang, V. Kale, J.E. Lancet, R.S. Komrokji, A.F. List, Phase II pilot study of oral dasatinib in patients with higher-risk myelodysplastic syndrome (MDS) who failed conventional therapy, Leuk. Res. 37 (2013) 300–304.

[37] S.E. Wheeler, E.M. Morariu, J.S. Bednash, C.G. Otte, R.R. Seethala, S.I. Chiosea, J.R. Grandis, Lyn kinase mediates cell motility and tumor growth in EGFRvIII-expressing head and neck cancer, Clin. Cancer Res. 18 (2012) 2850–2860.

[38] T. Force, K.L. Kolaja, Cardiotoxicity of kinase inhibitors: the prediction and translation of preclinical models to clinical outcomes, Nat. Rev. Drug Discov. 10 (2011) 111–126.

[39] A.L. Hopkins, C.R. Groom, A. Alex, Ligand efficiency: a useful metric for lead selection, Drug Discov. Today 9 (2004) 430–431.

[40] G.M. Keserue, G.M. Makara, The influence of lead discovery strategies on the properties of drug candidates, Nat. Rev. Drug Discov. 8 (2009) 203–212.

[41] C. Abad-Zapatero, J.T. Metz, Ligand efficiency indices as guideposts for drug discovery, Drug Discov. Today 10 (2005) 464–469.

[42] C. Abad-Zapatero, Ligand efficiency indices for effective drug discovery, Expert Opin. Drug Discov. 2 (2007) 469–488.

[43] P.D. Leeson, B. Springthorpe, The influence of drug-like concepts on decision-making in medicinal chemistry, Nat. Rev. Drug Discov. 6 (2007) 881–890.

[44] R.K. Kancha, N. von Bubnoff, C. Peschel, J. Duyster, Functional analysis of epidermal growth factor receptor (EGFR) mutations and potential implications for EGFR targeted therapy, Clin. Cancer Res. 15 (2009) 460–467.

[45] A. Ullrich, L. Coussens, J.S. Hayflick, T.J. Dull, A. Gray, A.W. Tam, J. Lee, Y. Yarden, T.A. Libermann, Human epidermal growth factor receptor cDNA sequence and aberrant expression of the amplified gene in A431 epidermoid carcinoma cells, Nature 309 (1984) 418–425.

[46] R. Bravo, J. Burckhardt, T. Curran, R. Muller, Stimulation and inhibition of growth by EGF in different A431 cell clones is accompanied by the rapid induction of c-fos and c-myc proto-oncogenes, EMBO J. 4 (1985) 1193–1197.

[47] M. Reiss, D.E. Brash, T. Munoz-Antonia, J.A. Simon, A. Ziegler, V.F. Vellucci, Z. Zhou, Status of the p53 tumor suppressor gene in human squamous carcinoma cell lines, Oncol. Res. 4 (1992) 349–357.

[48] T. Soonthornthum, H. Arias-Pulido, N. Joste, L. Lomo, C. Muller, T. Rutledge, C. Verschraegen, Epidermal growth factor receptor as a biomarker for cervical cancer, Ann. Oncol. 22 (2011) 2166–2178.

[49] M. Scheffner, K. Munger, J.C. Byrne, P.M. Howley, The state of the p53 and retinoblastoma genes in human cervical carcinoma cell lines, Proc. Natl. Acad. Sci. U. S. A. 88 (1991) 5523–5527.

[50] M. Eiblmaier, L.A. Meyer, M.A. Watson, P.M. Fracasso, L.J. Pike, C.J. Anderson, Correlating EGFR expression with receptor-binding properties and internalization of 64Cu-DOTA-cetuximab in 5 cervical cancer cell lines, J. Nucl. Med. 49 (2008) 1472–1479.

[51] D.T. Hendricks, R. Taylor, M. Reed, M.J. Birrer, FHIT gene expression in human ovarian, endometrial, and cervical cancer cell lines, Cancer Res. 57 (1997) 2112–2115.

[52] S. Bellone, G. Frera, G. Landolfi, C. Romani, E. Bandiera, G. Tognon, J.J. Roman, A.F. Burnett, S. Pecorelli, A.D. Santin, Overexpression of epidermal growth factor type-1 receptor (EGF-R1) in cervical cancer: implications for Cetuximab-mediated therapy in recurrent/metastatic disease, Gynecol. Oncol. 106 (2007) 513–520.

[53] A.C. Nichols, J. Yoo, D.A. Palma, K. Fung, J.H. Franklin, J. Koropatnick, J.S. Mymryk, N.N. Batada, J.W. Barrett, Frequent mutations in TP53 and CDKN2A found by next-generation sequencing of head and neck cancer cell lines, Arch. Otolaryngol. Head Neck Surg. 138 (2012) 732–739.

[54] V. Patel, A. Ramesh, J.L. Traicoff, G. Baibakov, M.R. Emmert-Buck, J.S. Gutkind, V. Knezevic, Profiling EGFR activity in head and neck squamous cell carcinoma by using a novel layered membrane Western blot technology, Oral Oncol. 41 (2005) 503–508.
[55] A.C. Pickhard, J. Margraf, A. Knopf, T. Stark, G. Piontek, C. Beck, A.L. Boulesteix, E.Q. Scherer, S. Pigorsch, J. Schlegel, W. Arnold, R. Reiter, Inhibition of radiation induced migration of human head and neck squamous cell carcinoma cells by blocking of EGF receptor pathways, BMC Cancer 11 (2011) 388–400.
[56] K.P. Orcutt, A.D. Parsons, Z.A. Sibenaller, P.M. Scarbrough, Y. Zhu, A. Sobhakumari, W.W. Wilke, A.L. Kalen, P. Goswami, F.J. Miller Jr., D.R. Spitz, A.L. Simons, Erlotinib-Mediated inhibition of EGFR signaling induces metabolic oxidative stress through NOX4, Cancer Res. 71 (2011) 3932–3940.
[57] S.S. Bacus, I. Stancovski, E. Huberman, D. Chin, E. Hurwitz, G.B. Mills, A. Ullrich, M. Sela, Y. Yarden, Tumor-inhibitory monoclonal antibodies to the HER-2/Neu receptor induce differentiation of human breast cancer cells, Cancer Res. 52 (1992) 2580–2589.
[58] L. Goestring, M. Malm, I. Hoeiden-Guthenberg, F.Y. Frejd, S. Staahl, J. Loefblom, L. Gedda, Cellular effects of HER3-specific affibody molecules, PLoS One 7 (2012) e40023.
[59] S. Sebban, M. Farago, D. Gashai, L. Ilan, E. Pikarsky, I. Ben-Porath, S. Katzav, Vav1 fine tunes p53 control of apoptosis versus proliferation in breast cancer, PLoS One 8 (2013) e54321.
[60] T. Takahashi, M.M. Nau, I. Chiba, M.J. Birrer, R.K. Rosenberg, M. Vinocour, M. Levitt, H. Pass, A.F. Gazdar, J.D. Minna, p53: a frequent target for genetic abnormalities in lung cancer, Science 246 (1989) 491–494.
[61] C.D. Little, M.M. Nau, D.N. Carney, A.F. Gazdar, J.D. Minna, Amplification and expression of the c-myc oncogene in human lung cancer cell lines, Nature 306 (1983) 194–196.
[62] S. Tanno, Y. Ohsaki, K. Nakanishi, E. Toyoshima, K. Kikuchi, Small cell lung cancer cells express EGFR and tyrosine phosphorylation of EGFR is inhibited by gefitinib ('Iressa', ZD1839), Oncol. Rep. 12 (2004) 1053–1057.
[63] T.H.K. Thvedt, E. Fuglseth, E. Sundby, B.H. Hoff, Enantioenriched 1-aryl-2-fluoroethylamines. Efficient lipase-catalysed resolution and limitations to the Mitsunobu inversion protocol, Tetrahedron 66 (2010) 6733–6743.
[64] J. Han, E. Sundby, B.H. Hoff, Solvent selection in synthesis of 4-(1-arylfluoroethoxy)quinazolines and thienopyrimidines, J. Fluorine Chem. 153 (2013) 82–88.
[65] C. Wang, A. Pettman, J. Basca, J. Xiao, A versatile catalyst for reductive amination by transfer hydrogenation, Angew. Chem. Int. Ed. 49 (2010) 7548–7552. S7548-1.
[66] D. Scopes, Pyrrolo[3,2-*e*][1,2,4]triazolo[1,5-a]pyrimidine Derivatives as Inhibitors of Microglia Activation and their Preparation and use for the Treatment of Diseases, WO 2011042497 A1, 14-4-2011.
[67] F. Levrat, H. Stoeckli-Evans, N. Engel, Enantiomeric excess determination of α-amino acids by 19F NMR spectroscopy of their (*N*,*N*-dimethyl-(2,2,2-trifluoro-1-phenylethyl)amine-C,N)palladium complexes, Tetrahedron: Asymmetry 13 (2002) 2335–2344.
[68] G. Fan, Y. Liu, Titanium-mediated cross-coupling reactions of imines with ketones or aldehydes: an efficient route for the synthesis of 1,2-amino alcohols, Tetrahedron Lett. 53 (2012) 5084–5087.
[69] P. Herdewijn, S. De Jonghe, L.-J. Gao, M.-Y. Jang, B. Vanderhoydonck, M.J.A. Waer, Y. Lin, J.F. Herman, T.A.M. Louat, Preparation of Bicyclic Heterocycles, Especially Thiazolopyrimidines, Oxazolopyrimidines, Thienopyrimidines and Purines for Treating Immune and Autoimmune Disorders Resulting from an Organ or Cells Transplantation, WO 2010103130 A2, 16-9-2010.